Title: Inositol phosphatase SHIP2 enables sustained MAP kinase activation by fibroblast growth factor via recruiting SRC kinases to the FGF-receptor signaling complex

Authors: Bohumil Fafilek[1,4¶], Lukas Balek[1¶], Michaela Kunova Bosakova[1,4], Miroslav Varecha[1,4], Alexandru Nita[1], Tomas Gregor[3], Iva Gudernova[1], Jitka Krenova[1], Somadri Ghosh[5], Martin Piskacek[2], Lucie Jonatova[1], Nicole H. Cernohorsky[1], Jennifer T. Zieba[6], Michal Kostas[7,8], Ellen Margrethe Haugsten[7,8], Jørgen Wesche[7,8], Christophe Erneux[4], Lukas Trantirek[2], Deborah Krakow[6,9,10], Pavel Krejci[1,4,11*]

Affiliations:

[1]Department of Biology, [2]Department of Pathological Physiology, Faculty of Medicine, [3]Central European Institute of Technology, Masaryk University, 62500 Brno, Czech Republic

[4]International Clinical Research Center, St. Anne's University Hospital, 65691 Brno, Czech Republic

[5]IRIBHM, Université Libre de Bruxelles, 1070 Bruxelles, Belgium

[6]Departments of Orthopaedic Surgery, [9]Human Genetics, and [10]Obstetrics and Gynecology, David Geffen School of Medicine, University of California Los Angeles, California 90095, USA

[7]Department of Tumor Biology, Institute for Cancer Research, The Norwegian Radium Hospital, 0379 Oslo, Norway

[8]Institute of Clinical Medicine, Faculty of Medicine, University of Oslo, 0379 Oslo, Norway

[11]Institute of Animal Physiology and Genetics of the CAS, 60200 Brno, Czech Republic

*correspondence to: krejcip@med.muni.cz

[¶]equal contribution

Abstract

Sustained activation of ERK MAP kinase drives pathologies caused by mutations in FGF-receptors (FGFRs), but the processes underlying these mechanisms remain unresolved. Using methodologies to identify novel mediators of FGFR signaling, we found that the inositol phosphatase SHIP2 (INPPL1) acts as an interactor and phosphorylation target of FGFR1, FGFR3 and FGFR4. Loss of SHIP2 effectively converted FGF-mediated sustained ERK activation into a transient signal, and rescued cell phenotypes triggered by pathologic FGFR-ERK signaling. Inhibition of inositol phosphatase activity did not impair SHIP2's association with FGFRs or FGF-mediated ERK activation, demonstrating that the adapter rather than catalytic activity of SHIP2 is important for maintenance of sustained ERK signal. SHIP2 recruited SRC-family kinases to the FGFRs, which assisted FGFRs in phosphorylation and assembly of protein complexes that relay signal to ERK. The findings showed that SHIP2 interacted with FGFRs, was phosphorylated by active FGFRs and regulated FGFR-ERK pathway at the level of adapter phosphorylation and PTPN11 recruitment. Thus, SHIP2 is an essential component of canonical FGF-FGFR signal transduction and a potential therapeutic target in FGFR-related disorders.

Key words: SHIP2; INPPL1; fibroblast growth factor; FGF; MAP kinase; adapter; signal transduction.

Introduction

Maintenance of tissue homeostasis depends on complex intercellular signaling networks that govern basic cell functions. The FGF system represents a major molecular toolkit of such cell-to-cell communications. Four FGFRs exist (FGFR1-4) and respond to extracellular signals delivered by at least 18 FGF ligands during development, life and disease. The importance of FGFR signaling is emphasized by their role in pathological functions. Numerous disorders arise from mutations, gene fusions, increased copy numbers, and other lesions affecting *FGFR* genes. These include cancer, developmental defects, and bone and skin disorders. The activating mutations in FGFR3 alone are associated with five severe skeletal dysplasias, nine types of cancer and two skin syndromes (*1–4*).

The ERK MAP kinase pathway is implicated in most cellular phenotypes regulated by FGF signaling. As an example, in human embryonic stem cells (hESC) or induced pluripotent cells, a balance of FGFR-mediated ERK activation was critical for either maintenance of undifferentiated phenotype, or induction of differentiation (*5–7*). Activation of ERK represents the predominant mechanism by which FGFRs trigger cell proliferation in fibroblasts, endothelial cells, myoblasts, mesenchymal stem cells, neural progenitors, and lung and lens epithelial cells (*1*). However, abnormal sustained ERK activation mediates FGFR oncogenic signaling in FGFR4-driven prostate cancer, BaF3 cells stably expressing the TEL-FGFR3 fusion protein, leukemic KG1 cells expressing the FOP2-FGFR1 fusion protein or KMS11 multiple myeloma cells overexpressing FGFR3 as a result of a t(4;14)(p16.3;q32) translocation (*8–11*). ERK drives much of the pathology underlying FGFR3-related skeletal dysplasias that include achondroplasia (ACH) and thanatophoric dysplasia (TD). Sustained ERK activation due to heterozygosity for FGFR3 activating mutations that cause ACH and TD, produced decreased chondrocyte proliferation, loss of extracellular matrix and altered chondrocyte differentiation (*12*, *13*). Similarly, increased ERK signaling mediated premature fusion of

synchondroses in the developing vertebrae producing narrowing of the spinal canal at the foramen magnum furthering skeletal complications seen ACH (*14*). Expression of constitutively-active MEK1 also leads to an ACH-like dwarfism in mice (*15*) supporting that downstream of ERK in the pathway, overexpression of MEK1 produced similar phenotypic consequences.

FGFRs recruit ERK pathway via adapter-mediated translocation of the RAS guanine nucleotide exchange factor SOS1 to the cell membrane. The FGFR substrate 2 (FRS2) represents a major adapter involved in this process. FGFRs phosphorylate FRS2 on at least six tyrosine residues that serve as binding sites for SOS1 complexed with GRB2, directing a substantial amount of SOS1 to the cell membrane where it activates RAS (*16*, *17*).

In chondrocytes or hESC, FGFR activation leads to strong FRS2 tyrosine phosphorylation and corresponding sustained ERK activation lasting for more than 8 hours (*18*). The processes regulating the maintenance of sustained ERK activity in FGFR signaling are poorly characterized, yet they lead to severe pathology. In this study, we show that FGFRs interacted with and phosphorylated the inositol phosphatase SHIP2 (or INPPL1), which in turn recruited SRC-family kinases to the FGFR signaling complex, where they assisted FGFR-mediated phosphorylation of FRS2 and GAB1 adapters that relayed the signal to ERK pathway. Loss of SHIP2 converted sustained FGF-mediated ERK activation into a transient signal, demonstrating that SHIP2 is an essential component of FGF signaling and necessary for the maintenance of FGF-mediated ERK activation.

Results

To further our understanding of FGFR signaling in cells, we used proteomics to identify proteins phosphorylated upon activation of endogenous FGFR2 and FGFR3 (*19*) signaling in cultured rat chondrosarcoma (RCS) chondrocytes. As detailed previously (*20*), the tyrosine

phosphorylated proteins were purified from cells treated with the FGF ligand FGF2 by immunoprecipitation with a pan-pTyr antibody, and subjected to tandem mass spectrometry. Inositol phosphatase SHIP2 was among the most frequent proteins phosphorylated at tyrosine upon FGFR activation, being found in 4/6 of the experiments carried out.

FGFRs interact with SHIP2 and target SHIP2 to focal adhesions

Both wildtype FGFR3 and its activating mutant FGFR3-K650M, associated with TD (*21*), co-immunoprecipitated with SHIP2 when expressed in 293T cells (Fig. 1A). FGFR3 induced SHIP2 phosphorylation at $Tyr^{986/7}$ and Tyr^{1135} in 293T cells (Fig. 1A) as well as in cell-free kinase assays utilizing recombinant FGFR3 as a kinase and recombinant SHIP2 as a substrate (Fig. 1B, lane 4). Addition of recombinant SHIP2 did not affect FGFR3 activity in a kinase assay, as demonstrated by no change in FGFR3 autophosphorylation in the presence of SHIP2 (Fig. 1C). Similarly, FGFR3 did not alter the inositol phosphatase activity of SHIP2, as demonstrated by a cell-free SHIP2 activity assay based on colorimetric detection of phosphate released during hydrolysis of phosphoinositide PtdIns(3,4,5)P3 to PtdIns(3,4)P2 (Fig. 1D). These experiments established that FGFR3 interacts with SHIP2 and acts as a SHIP2 kinase. The experiments also show that FGFR3-SHIP2 interaction does not affect the catalytic activity of either protein.

SHIP2 contains three clearly distinguished domains according to structural data available at the PDB database (ww.pdb.org): a N-terminal SRC-homology 2 (SH2) domain (PDB: 2MK2), a central inositol phosphatase (PS) domain (PDB: 4A9C) and a sterile alpha motif (SAM) domain located at the C-terminus (PDB: 2K4P). In addition, we identified two proline rich (PR) domains in SHIP2, located between residues 123-160 (PR1), and 935-1105 (PR2) in human SHIP2 (Fig. 2A). A series of C-terminally V5-tagged truncated SHIP2 variants was generated and subjected to co-immunoprecipitations with FGFR3. Deletion of the PS or PR1

domains produced no effect on SHIP2 co-immunoprecipitation with FGFR3 (Fig. 2, B and C). In contrast, individual deletion of SH2 or SAM domains substantially impaired FGFR3-SHIP2 association (Fig. 2, D and E; arrows), suggesting a bipartite SHIP2-FGFR3 interaction involving both SH2 and SAM domains. No co-immunoprecipitation of wildtype SHIP2 with catalytically-inactive K508M mutant of FGFR3 (Fig. 2F), suggesting that SHIP2 associates preferentially with active FGFR3.

Having found that SHIP2 interacts with FGFR3, we asked whether it associates with other FGFRs. In 293T cells, SHIP2 co-immunoprecipitated with FGFR1 and FGFR4; no interaction with FGFR2 was found (Fig. 3A). We next used osteosarcoma U2OS cells stably expressing C-terminally GFP-tagged FGFR1 to probe SHIP2 association with FGFR1. By proximity ligation (PLA) assay, an association of endogenous SHIP2 with FGFR1 was found using SHIP2 antibody in combination with GFP antibody (Fig. 3, B, C). Similar data were obtained using PLA with FGFR1 and SHIP2 antibodies (Fig. 3, D, C). No significant PLA signal was found in isogenic negative controls to both experiments, i.e. U2OS cells stably expressing FGFR1-HA (for GFP:SHIP2 PLA), and U2OS cells stably expressing FGFR4-GFP (for FGFR1:SHIP2 PLA).

Treatment of RCS cells with FGF2 triggered phosphorylation of endogenous SHIP2 at $Tyr^{986/7}$ (Fig. 4A), and targeted SHIP2 to the cell periphery where it partially co-localized with the focal adhesion marker vinculin (Fig. 4, B, C and E). Similar translocation and association with peripheral focal adhesions were observed for the p130CAS signaling adapter (Fig. 4, D and E), which was previously found phosphorylated at multiple tyrosines in FGF2-treated RCS cells (*20*). Because SHIP2 and p130CAS interacted with FGFR3 and are FGFR3 substrates, it is likely that they are phosphorylated by the FGFR3 and transit to focal adhesions together. Supporting this hypothesis was the finding that p130CAS and SHIP2 interact via the substrate domain of p130CAS and localize to lamellipodia together (*22*).

SHIP2 is part of the integrin adhesome and is known to interact with various cytoskeletal proteins (*23*). Previous data obtained in human fibroblasts show that cell migration is significantly decreased in SHIP2 *null* fibroblasts derived from opsismodyplasia patients (*24*). To establish the role of SHIP2 in FGF-mediated cell migration, we used the CRISPR/Cas9 system to disrupt the *Ship2* gene in RCS cells. Four RCS clones with *Ship2* loci targeted by CRISPR/Cas9 (SHIP2^{Crispr} cells) were selected, their genotypes characterized by sequencing and their SHIP2 expression determined by western blot (clone names and genotypes: Ship2$^{c-/-}$, Ship2$^{a+/-}$, Ship2$^{g-/-}$ and Ship2$^{f+/-}$) (Fig. 4F). Using fibronectin-coated glass bottom chambers, we compared the cell migration velocity between wildtype and SHIP2^{Crispr} cells. In the presence of 10% serum, the migration was inhibited in two SHIP2^{Crispr} cell lines, when compared with wildtype cells (Fig. 4G). In contrast, SHIP2 deletion lead to significantly increased migration in cells treated with FGF2 in the absence of serum. Therefore, SHIP2 controls cell migration in RCS cells, and acts as a negative regulator of FGF-mediated migration.

SHIP2 deletion rescues cellular phenotypes triggered by FGFR activation

RCS cells represent a well-established chondrocyte model to study pathologic increased FGFR3 signaling as seen in ACH or TD caused by activating FGFR3 mutations. The cells respond to activation of endogenous FGFR signaling with complex changes in cell behavior manifested by growth arrest, diminished collagen and proteoglycan extracellular matrix (ECM), induction of premature senescence and alteration in cell shape (*12*, *13*, *25*, *26*). When compared to wildtype cells, the SHIP2^{Crispr} cells responded to FGF2 with significantly less potent growth arrest (Fig. 5A). This phenotype was not due to clonal variation, because three randomly selected RCS clones with wildtype SHIP2 genotypes responded to FGF2 with growth arrest comparable to wildtype cells (Fig. 5, B and C). The SHIP2^{Crispr} cells also showed less of the FGF2-mediated ECM loss, determined by western blot for collagen 2 and alcian blue

staining for sulfated proteoglycans, respectively (Fig. 5, D and E, and fig. S1A). Finally, FGF-mediated induction of premature senescence was also less pronounced in SHIP2^{Crispr} cells compared to wildtype controls, as demonstrated by western blot for presence of the senescence marker caveolin 1 (Fig. 5D) (*12*). These experiments established that SHIP2 deletion renders RCS cells less responsive to FGF stimulus during multiple FGF-mediated cellular phenotypes. In contrast, SHIP2 deletion did not affect FGF-induced changes in cellular shape, manifested as cell flattening and enlargement (Fig. 5F and fig. S1B) due to cytoskeletal remodeling with abundant formation of actin stress fibers (Fig. 5G) (*18*). The SHIP2 translocation to peripheral focal adhesions in response to FGF2 (Fig. 4, B and C) is therefore not essential for FGF-mediated cell spreading and cytoskeletal remodeling.

SHIP2 deletion converts FGF-mediated sustained ERK activation into a transient signal

First, we asked whether the lack of response to FGF2 in SHIP2^{Crispr} cells may simply stem from FGFR downregulation. No substantial changes in FGFR2 or FGFR3 protein amounts were found among wildtype and SHIP2^{Crispr} cells, ruling-out this possibility (fig. S2). Because sustained ERK activation accounts for the majority of cellular phenotypes triggered by FGF in RCS cells (*27*), we next examined the kinetics of ERK activity in SHIP2^{Crispr} cells. All four SHIP2^{Crispr} cell lines showed markedly impaired FGF-mediated ERK activation, which progressed with time, resulting in almost completely diminished ERK signal in cells treated with FGF2 for over four hours (Fig. 6A and fig. S3, A to C). In contrast, wildtype cells maintained phosphorylated ERK amount for at least 10 hours. Thus, the SHIP2^{Crispr} cells responded to FGF-mediated ERK activation normally but failed to maintain ERK activity over prolonged periods of time. The defective maintenance of ERK activation clearly explains the rescue of the FGF-mediated changes in cell behavior observed in SHIP2^{Crispr} cells.

We next asked whether the defect in FGF-mediated ERK activation in SHIP2^{Crispr} cells

may be restored by addition of SHIP2 protein. Western blot with recombinant SHIP2 was used to determine the amount of SHIP2 protein in cells (287,546±37,305 molecules/cell, mean±SEM; n=9) (Fig. 6B). Two SHIP2^{Crispr} cell lines were microinjected with amount of recombinant SHIP2 (recSHIP2) of approximately 1/10th (~25,000 molecules/cell) of the endogenous SHIP2, together with dTomato transcriptional reporter to ERK activity (pKrox24(MapErk)^{dTomato}) (*28*) (Fig. 6C). Cells were treated with FGF2 and the induction of dsTomato expression was analyzed 24 hours later and plotted. Injection of recSHIP2 increased the FGF ability to activate ERK in the SHIP2^{Crispr} cells (Fig. 6, D and E).

To test whether other receptor tyrosine kinases also require SHIP2 to activate ERK, RCS cells were transfected with full-length wildtype human Tropomyosin receptor kinase (TRKA) or Epidermal Growth Factor Receptor (EGFR), and treated with the TRKA and EGFR ligands NGF and EGF, respectively. The TRKA- or EGFR-mediated ERK activation was compared between wildtype cells and two SHIP2^{Crispr} cell lines. No substantial differences in ERK activation were found among wildtype and SHIP2^{Crispr} cells (fig. S4), suggesting that, TRKA and EGFR do not require SHIP2 for ERK activation, conferring specificity to FGFR signaling.

FGFRs relay their signal to the ERK pathway via adapters such as FRS2 and GAB1, which undergo tyrosine phosphorylation upon FGF treatment of cells and complex with PTPN11 (SHP2) adapter/tyrosine phosphatase to activate the RAS-ERK signaling module. FGF2 triggered abundant tyrosine phosphorylation of FRS2(Tyr^{436}) and GAB1(Tyr^{627}) in RCS cells (*27*) (Fig. 6A and fig. S3, A to C), which was impaired in SHIP2^{Crispr} cells. These data suggest that the defect in ERK activation in SHIP2^{Crispr} cells may stem from poor recruitment of PTPN11 onto underphosphorylated adapters. We could not immunoprecipitate GAB1 from RCS cells (despite multiple attempts) due to technical difficulties. However, the FRS2-PTPN11 co-immunoprecipitation experiments showed impaired association of FRS2 with PTPN11 upon FGF2 treatment in SHIP2^{Crispr} cells, when compared to wildtype cells (Fig. 6F and fig.

S3D).

SHIP2 promotes association of SRC kinases with FGFR3

The SRC-family kinases BLK, FGR, FYN, HCK, LCK, LYN and YES were amongst the most frequent proteins found in MS analyses of the FGFR3 interactome (*20*). The FGFR3 association with FYN, LYN, FGR, BLK, and LCK was confirmed by co-immunoprecipitations carried out in 293T cells (Fig. 7A and fig. S5). The bimolecular fluorescence complementation (BiFC) was used to visualize the FGFR3 and FYN interaction in cells. For this analysis, LYN cDNA was C-terminally fused with cDNA encoding for Venus N-terminal 1-158 amino acid residues (*29*) (LYN-V1), while FGFR3 cDNA was fused to Venus cDNA encoding its C-terminal 159-239 amino acid residues (FGFR3-V2). Figure 7, B and C demonstrates the direct interaction of FGFR3 with LYN in 293T cells.

Inhibition of endogenous SRC catalytic activity by two unrelated chemical inhibitors (AZM475271, A419259) abolished ERK activation triggered by addition of exogenous FGF2, in both RCS and 293T cells (Fig. 7, D and E). The ERK inhibition was accompanied by the inhibition of FRS2 phosphorylation, suggesting that SRC kinases are recruited to FGFRs and participate in FGFR-mediated adapter phosphorylation and ERK activation.

Having established that SHIP2 deletion and SRC inhibition both impaired FGF-mediated ERK activation, we speculated that SHIP2 promotes association of SRC kinases with FGFRs. The PLA was used to probe FGFR3 interaction with the SRC kinase YES in RCS cells of differing *Ship2* backgrounds. Expression of FGFR3 in RCS cells lead to its spontaneous activation (Fig. 7F), and association with co-expressed YES at the cell membrane (Fig. 7, G and H). This association was reduced by 40% and 61% in the two tested SHIP2^{Crispr} cell lines (Fig. 7I), suggesting that SHIP2 facilitates FGFR3 interaction with SRC kinases.

Inositol phosphatase activity of SHIP2 is not necessary for FGF-mediated ERK activation

The truncated SHIP2 variant lacking the entire inositol phosphatase domain (SHIP2-ΔPS) interacts normally with FGFR3 (Fig. 2B). Similarly, FRS2, LYN, LCK and FGR co-immunoprecipitated normally with SHIP2-ΔPS or with the phosphatase-defective SHIP2 triple mutant (P686A/D690A/R691A) (SHIP2-PD) (*30*) (Fig. 8, A to C, and fig. S6). Thus, the interaction with FGFR3 or members of its signaling complex does not require SHIP2's inositol phosphatase domain or its catalytic activity.

To test whether the catalytic function is required for the role of SHIP2 in FGF-ERK signaling, RCS cells were treated with a chemical inhibitor of SHIP2 inositol phosphatase activity (AS1949490) (*31*). Since SHIP2 acts as a negative regulator of PI3K/AKT pathway, the AS1949490 should increase AKT signaling. AS1949490 treatment produced no changes in basal phosphorylation of AKT(Ser^{473}) or its direct substrate FoxO1(Thr^{24}) (*32*) in FGF2-naïve cells. However, the well documented inhibition of AKT activity (and corresponding lack of FoxO1 phosphorylation) by prolonged FGFR signaling in RCS cells (*33*, *34*) was prevented by AS1949490 (Fig. 8D, arrows), confirming that the inhibition of SHIP2 upregulated AKT activity. AS1949490 did not alter FGF-mediated FRS2 phosphorylation and, surprisingly, enhanced rather than suppressed the FGF-mediated ERK phosphorylation (Fig. 8D). Next, ERK activity in RCS cells was monitored by a pKrox24(MapErk)^{Luciferase} reporter designed to record quantitative changes in ERK pathway activation by FGF signaling (*19*). The FGF-mediated pKrox24 transactivation was enhanced in cells transfected with wildtype SHIP2, compared to untransfected controls (~13 fold vs. ~9 fold) (Fig. 8E). Interestingly, the pKrox24 transactivation was enhanced up to ~17 fold in cells transfected with SHIP2-ΔPS, altogether suggesting that lack of SHIP2 catalytic activity does not account for diminished FRS2 phosphorylation and ERK activation in FGF-treated SHIP2^{Crispr} cells. Thus, the loss of SHIP2 leading to decreased FGF-mediated ERK activation likely results from its role as a physical

adaptor in the signalling cascade.

Discussion

Most of the twenty established receptor tyrosine kinases (RTK) families use the ERK pathway as major effector of their signal transduction. The magnitude and duration of ERK activation appear critical for cell decisions during the physiological processes regulated by RTKs. In PC12 pheochromocytoma cells for instance, the transient ERK activation by EGFR leads to increased proliferation in contrast to growth arrest and neuronal differentiation induced by sustained ERK activation via TRK signaling (*35*, *36*). In pathological conditions, sustained ERK activation is almost invariantly the major driver of cell phenotypes caused by RTK deregulation. The FGFRs are no exception from this paradigm, but the mechanisms associated with constant ERK activation in FGFR signaling remain unclear. Deepening our understanding of the mechanisms associated with ERK activation, will aid in progress towards treatments for FGFR-related conditions.

FGFRs relay their signal to ERK via adapters such as FRS2. FGFRs phosphorylate FRS2 at several tyrosine residues that serve as binding sites for GRB2-SOS1 ($Tyr^{196/306/349/392}$) and PTPN11-GRB2-SOS1 ($Tyr^{436/471}$) complexes, directing SOS1 guanine nucleotide exchange factor to the cell membrane where it activates RAS (*16*, *17*). Adapters not only relay the signal, but also act as its amplifiers, since the phosphorylation of several adapter molecules by single FGFR substantially increases the docking interface for cytoplasmic SOS1 at the cell membrane. Thus, RTK families such as FGFR or TRK that use adapters, tend to produce higher and longer ERK activation when compared to RTKs that engage their downstream signaling directly (*37*).

Although FGFRs induce strong ERK activation in general, the actual magnitude and duration of ERK activity fluctuates substantially among different cell types, ranging from 1-2 hours in fibroblasts to persistent signal for at least 24 hours in chondrocytes (*33*). The

mechanisms maintaining this ERK activity are poorly understood. According to the existing paradigm, FGFR activation leads its rapid internalization and degradation. This is followed by a period where a given cell is insensitive to FGF, before new FGFR molecules become present at the cell surface (*4*, *38–40*). In some pathologies, continuous presence of FGFRs at the cell surface contribute to sustained ERK activity. These include gastric and lung cancer cells, where *Fgfr1* and *Fgfr2* are frequently amplified, leading to constant FGFR expression or multiple myeloma, where FGFR3 is overexpressed as a result of t(4;14)(p16.3;q32) translocation placing an immunoglobulin promotor upstream of the *Fgfr3* gene (*41–43*). Although the high abundance of FGFR3 are part of the chondrocyte differentiation program, experimental evidence demonstrated rapid FGFR3 downregulation following its activation (*26*). Thus, the persistence of FGFRs at the membrane is unlikely to account for sustained ERK activation in chondrocytes.

The adaptors used for ERK activation may attenuate the ERK signal. FRS2 represents such a site of potent negative feedback. First, tyrosine phosphorylated FRS2 mediates the interaction of ubiquitin ligase cCBL with FGFR, leading to its ubiquitin-mediated degradation (*44*). Second, active ERK phosphorylates FRS2 at multiple threonine residues adjacent to the phosphorylated tyrosines, leading to diminished PTPN11-GRB2-SOS1 recruitment and downregulation of ERK activity (*45*, *46*). The components of the ERK-FRS2 negative feedback loop exists in chondrocytes, but there is no corresponding downregulation of ERK activity (*27*). Moreover, analyses of transcriptional changes triggered by FGFR activation in chondrocytes (*18*), demonstrated a potent induction of ERK phosphatase DUSP6 as well as members of the Sprouty family of RAS-ERK pathway inhibitors (*47*, *48*). Thus, FGF-mediated ERK activation persists for many hours despite the induction of negative feedback mechanisms, suggesting the existence of other cellular processes capable of overriding established negative feedback mechanisms. Our study describes one such mechanistic pathway, linking the inositol

phosphatase SHIP2 to the FGFR signaling complex in regulation of sustained ERK activation. Our findings showed that SHIP2 interacted with FGFRs, was phosphorylated by active FGFRs and regulated the FGFR-ERK pathway at the level of adapter phosphorylation and PTPN11 recruitment (Fig. 8F).

The SRC kinases are known to participate in a pleiotropic array of FGF-regulated events including cell proliferation, shape changes, migration, adhesion, and differentiation (*49–56*). The mechanism of FGFR-mediated recruitment of SRCs is somewhat unclear, although earlier studies demonstrate direct SRC interaction with FGFRs, or recruitment via FRS2 (*57–59*). Similarly, although most of the cellular phenotypes caused by FGF-SRC signaling are dependent on ERK (*49, 60*), it is not clear how SRCs mechanistically integrate into the FGF-ERK pathway. We showed that SRC kinases are recruited to the FGFR signaling complex by SHIP2. Inhibition of SRC activity abolished FGF-mediated ERK activation and FRS2 phosphorylation, suggesting that SRCs assist FGFRs in adapter phosphorylation and signal relay to the ERK pathway, together enabling for a robust, negative feedback-resistant relay of the FGFR signal to the RAS-ERK pathway. Our experiments thus establish SHIP2 as an essential component of canonical FGFR signaling that enables sustained FGFR-mediated ERK activation by recruiting SRC kinases to the FGFR signaling complex (Fig. 8F).

The major physiological function attributed to SHIP2 is the regulation of insulin signaling. *Ship2* knock-out mice showed increased sensitivity to insulin, causing hypoglycaemia, deregulated expression of genes involved in liver gluconeogenesis, and perinatal death (*61*). A later study did not confirm such a severe phenotype, but reported a resistance of *Ship2*$^{-/-}$ animals to weight gain, due to the decreased cellular response to insulin (*62*). In addition to altered insulin signaling, the *Ship2*$^{-/-}$ mice are approximately half in size of their wildtype littermates, suggesting a role of SHIP2 in regulation of axial and appendicular skeleton. Interestingly, loss of function mutations in *SHIP2* cause opsismodysplasia, an

autosomal recessive skeletal dysplasia characterized by severe shortening of all the appendicular bones with radiographic evidence of endochondral ossification delay, extremely short hands, poor mineralization flattening of the spine, and severe midface hypoplasia (*63*–*65*). Histologic analyses of cartilage growth plate morphology due to mutations in SHIP2 showed poorly organized zone of proliferating chondrocytes, nearly absent zone of hypertrophic chondrocytes and increased vascular invasion (*66*, *67*).

Molecular analyses demonstrated that the negative role of SHIP2 on metabolic insulin signaling is caused by SHIP2-mediated inhibition of PI3K/Akt signaling (*30*, *62*). This was mediated by SHIP2 dephosphorylation of membrane phosphoinositide PtdIns(3,4,5)P3 to PtdIns(3,4)P2, which reduced AKT binding sites, restricting recruitment and subsequent AKT activation by PDK1 (3-phosphoinositide-dependent protein kinase-1) at the cell membrane (*68*). Similar to the role of SHIP2 in insulin metabolism, opsismodysplasia stems from the lack of catalytic SHIP2 function since several patients with opsismodysplasia have been shown to harbor missense mutations localized in the catalytic domain (*69*, *70*). Because IGF signals primarily through the PI3K/AKT pathway (*71*) it is likely that the mutations in *SHIP2* producing opsismodyplasia do so through deregulation of IGF-AKT mitogenic signaling. Impaired insulin-like growth factor (IGF) signaling is major growth promoting signal for skeleton (*72*). Analyses of IGF or its receptor IGF-1R knockout models showed growth retardation with poor mineralization and an abnormal cartilage growth plate that shared similarities to the human *SHIP2*$^{-/-}$ cases that included disorganized proliferating chondrocytes and shortened hypertrophic zone, supporting that hypothesis abnormal insulin signaling effects the growth plate (*73*, *74*). Beyond PI3K/AKT signaling, IGF-1R interacts with the Parathyroid hormone-related peptide/Indian hedgehog pathway (PTHrP/IHH) adding complexity to direct and indirect effects on loss of SHIP2 on the chondrocyte cellular behavior that now includes regulatory effects on FGFR signaling (*74*).

However, the SHIP2-mediated regulation of FGF signaling in chondrocytes appears to be independent of SHIP2 catalytic activity and the AKT pathway. First, deletion or downregulation of SHIP2 in SHIP2^{Crispr} cells did not increase AKT signaling as expected when assuming that the role of SHIP2 is solely the inhibition of the PI3K/AKT pathway. Second, chemical inhibition of SHIP2 phosphatase activity increased AKT phosphorylation but did not downregulate FGF-mediated ERK activation or adapter phosphorylation. Third, genetic inactivation or deletion of the SHIP2 catalytic domain did not affect its association with the FGFR signaling complex. It thus appears that SHIP2's catalytic function is important for mitogenic IGF signaling in growth plate cartilage, whereas its adapter function is critical for the growth inhibitory signaling of FGFR3 in the same tissue. Further experiments should unravel the interesting and yet unknown biology behind how the two growth factor systems, i.e. IGF and FGF, integrate SHIP2 into their downstream signaling in order to achieve their opposing effects on cell proliferation. These studies should also illuminate the therapeutic potential of modulation of SHIP2 activity in developmental conditions caused by activating mutations in FGFRs.

Material and Methods

Cell culture, vectors, transfection and luciferase assay

293T (ATCC, Manassas, VA), U2OS and RCS cells (obtained from B. de Crombrugghe) (*75*) were propagated in DMEM media, supplemented with 10% FBS and antibiotics (Invitrogen, Carlsbad, CA). To obtain cells stably expressing FGFR4-GFP, U2OS cells were transfected with pEGFP-N1-FGFR4 plasmid (*76*) using Fugene liposomal transfection reagent according to the manufacturer's protocol. Clones were selected with 1 mg/ml geneticin and their FGFR4-GFP expression levels were analyzed by immunofluorescence and western blot. A homogenous clone with moderate FGFR4-GFP expression level was chosen for further studies. U2OS cells

stably expressing FGFR1-GFP and FGFR1-BirA-HA were described recently (*77*). For cell migration assay, cells were plated on fibronectin coated 8 chambered μ-slide wells and allowed to migrate for 15 hours as reported before (*24, 78*). Cells were analyzed with Leica DM6000B microscope, using 10X magnification objective for live-cell imaging. Each cell was tracked over the period of time using the manual tracking plugin of the ImageJ software. FGF2, NGF and EGF were from RnD Systems (Minneapolis, MN), heparin was from Sigma-Aldrich (St. Louis, MO), AZM475271, A419259 and AS1949490 were from Tocris Bioscience (Ellisville, MO). Cells were transfected using FuGENE6 reagent according to manufacturer's protocol (Promega, Madison, WI). Vectors expressing FGFR3 were described elsewhere (*19*). Vectors expressing BLK, FYN, FGR, LYN, LCK and YES were obtained from ImaGenes (Berlin, Germany); EYFP vector was from Clontech (Mountain View, CA). For generation of truncated SHIP2 variants, the C-terminal Myc-DDK tag in pCMV6-hShip2 vector (OriGene, San Diego, CA) was replaced by V5-HIS tag using NEBuilder HiFi DNA assembly kit (New England Biolabs, Ipswich, MA). Truncated SHIP2 constructs were generated by PCR mutagenesis. Catalytically-inactive 5'-phosphatase-defective (PD) SHIP2 was created by introducing P686A, D690A and R691A substitutions into the inositol phosphatase domain via site-directed mutagenesis (Agilent, Santa Clara, CA). For dual-luciferase assay, the pKrox24(2xD-E_inD)Luc firefly luciferase reporter (*19*) was transfected together with the pTK-RL vector (Promega) in 3.2/1 (μg DNA) ratio. Cells were treated with FGF2 for 24 hours and the luciferase amount was determined using dual luciferase assay (Promega).

Microinjection

Cells were microinjected using Femtojet 4i microinjector with micromanipulator Injectman 4 (Eppendorf, Germany). Each cell was injected with 200 fl of PBS containing ~25,000 molecules of recombinant SHIP2 (recSHIP2; SignalChem, Canada) together with fluorescence

marker Dextran Alexa Fluor™ 647 (Thermo Fisher Scientific, USA) and 100 molecules of pKrox24(MapErk)^{dTomato} reporter developed for detection of ERK activity (*79*). Samples were treated for 24 hours with 10 ng/ml FGF2 to activate ERK pathway. Fixed cells were imaged for pKrox24 transactivation, using automatic microscope TissueFAXsi (TissueGnostics, Austria) with 20x air objective. Percentages of injected cells positive for dTomato were determined by Fiji free software.

Immunoprecipitation, western blot and activity assays

Cells were lysed in buffer containing 50 mM Tris-HCl pH 7.4, 150 mM NaCl, 0.5% NP-40, 0.25% sodium deoxycholate, 2 mM EDTA and 1 mM Na_3VO_4, supplemented with protease inhibitors. Lysates were cleared by centrifugation and supernatants were incubated for 1 hour with antibodies. Immunocomplexes were collected on A/G-agarose (Santa Cruz Biotechnology, Santa Cruz, CA) in overnight incubation. For the western blot, cell lysates were resolved by SDS-PAGE, transferred onto a PVDF membrane and visualized by chemiluminiscence (Thermo Scientific, Rockford, IL). Table S1 lists antibodies used in the study. For kinase assays, 200 ng of recombinant FGFR3 was incubated for 30 minutes at 30°C with recombinant SHIP2 (SignalChem, Richmond, CA) as a substrate, in 50 μl of kinase buffer (60 mM HEPES pH 7.5, 3 mM $MgCl_2$, 3 mM $MnCl_2$, 10 μM Na_3VO_4, 1.2 mM DTT) supplemented with 10 μM ATP. For the SHIP2 activity assay, 300 ng FGFR3 and 400 ng SHIP2 was incubated with 50 μM PIP3 (Echelon Biosciences, Salt Lake City, UT) for 30 minutes at 30°C. The reaction was then incubated with Biomol Green Reagent (Enzo Life Sciences, Exeter, United Kingdom) and optical density at 620 nm was determined by spectrophotometer. Crystal violet staining was carried out as described before (*80*).

CRISPR/Cas9

SHIP2 ablation in RCS cells using CRISPR/Cas9 technology was carried out as described (*81*). CHOPCHOP tool was used to design sgRNAs for a pair of SpCas9n (D10A) nickases, which targeted 5´-GTGTGGGGCACCGAGTCCCG-3´, 5´-GTCACGGTGATACCAGGCAG-3´ sites in the first exon of the *Ship2* gene (*82*). Together with a pair of Crispr/Cas9n plasmids, RCS cells were electroporated also with a GFP based Crispr Reporter (designed GReP, a generous gift from V. Korinek) where the targeted sequence was cloned amidst the GFP coding sequence. Successful targeting restored the GFP-reading frame and GFP-positive cells were manually picked and expanded. Individual clones were screened on western blot for SHIP2 presence, and the targeted locus was PCR amplified using 5´-AGCCTCCACTCCAAGCTTCC-3´, 5´-AAGGTCTCCACTCACGGTGG-3´, inserted into pGEM T-Easy vector (Promega) and sequenced for determination of *Ship2* genotype.

Immunocytochemistry, alcian blue staining and proximity ligation assay (PLA)

Cells were fixed in 4% paraformaldehyde and incubated with primary antibodies at 4°C overnight. Secondary antibodies were Alexa Fluor 488/594-conjugated secondary antibodies (Life Technologies, Grand Island, NY). Polymerized actin was visualized using AlexaFluor 594-conjugated Phalloidin (Life Technologies) and vinculin stained with vinculin-FITC antibody according to the manufacturer's protocol (Sigma). For Duolink® PLA (Sigma), cells were transfected with vectors expressing FGFR3-Flag together with YES-YFP or YFP, fixed and stained according to manufacturer´s protocol. PLA events were calculated in YFP-positive cells in 3D and normalized to YFP signal. For alcian blue staining, cells were fixed with paraformaldehyde, stained with 1% alcian blue (Sigma) and mounted. Images were taken using a confocal inverted microscope Carl Zeiss LSM 700 (Jena, Germany) with 63x oil immersion objective. Images shown in Figures 3B-E and 4H represent maximum projections of several acquired z-sections. Brightfield images of alcian blue samples (Fig. 4F and fig. S1A) were

taken using Olympus microscope IX71 (Tokyo, Japan). Phase contrast images were taken using Carl Zeiss Axio Observer microscope. The contrast, brightness, and gamma were adjusted.

Statistical analysis

We used Welch's t-test for statistical analysis of significance due to unequal variances in our samples. Where appropriate we used Bonferroni's correction of p values. Statistical methods were discussed and approved by renowned biostatistician.

Supplementary Materials

Supplementary figure S1. *Ship2* deletion or downregulation by CRISPR/Cas9 impairs FGFR3 ability to induce extracellular matrix (ECM) degradation but not cell spreading in RCS cells.

Supplementary figure S2. *Ship2* deletion or downregulation by CRISPR/Cas9 does not affect FGFR2 and FGFR3 abundance in RCS cells.

Supplementary figure S3. Deletion or downregulation of *Ship2* impairs FGF2-mediated adapter phosphorylation and activation of ERK MAP kinase.

Supplementary figure S4. No substantial impairment of NGF- or EGF-mediated in ERK activity was found in $SHIP2^{Crispr}$ cells.

Supplementary figure S5. FGFR3 interacts with SRC-family kinases FYN, LYN, FGR and BLK.

Supplementary figure S6. FGR associates with both wild-type (WT) and catalytically-inactive (PD) SHIP2.

Supplementary table S1. Antibodies used in the study.

Supplementary table S2. Expression vectors used in the study.

References and Notes

1. P. Krejci, The paradox of FGFR3 signaling in skeletal dysplasia: why chondrocytes growth arrest while other cells over proliferate. *Mutat. Res. Rev. Mutat. Res.* **759**, 40–8 (2014).
2. D. M. Ornitz, P. J. Marie, Fibroblast growth factor signaling in skeletal development and disease. *Genes Dev.* **29**, 1463–1486 (2015).
3. L. Bonafe, V. Cormier-Daire, C. Hall, R. Lachman, G. Mortier, S. Mundlos, G. Nishimura, L. Sangiorgi, R. Savarirayan, D. Sillence, J. Spranger, A. Superti-Furga, M. Warman, S. Unger, Nosology and classification of genetic skeletal disorders: 2015 revision. *Am. J. Med. Genet. Part A* **167**, 2869–2892 (2015).
4. J. Wesche, K. Haglund, E. M. Haugsten, Fibroblast growth factors and their receptors in cancer. *Biochem. J.* **437**, 199–213 (2011).
5. P. Dvorak, D. Dvorakova, S. Koskova, M. Vodinska, M. Najvirtova, D. Krekac, A. Hampl, Expression and potential role of fibroblast growth factor 2 and its receptors in human embryonic stem cells. *Stem Cells* **23**, 1200–11 (2005).
6. J. Li, G. Wang, C. Wang, Y. Zhao, H. Zhang, Z. Tan, Z. Song, M. Ding, H. Deng, MEK/ERK signaling contributes to the maintenance of human embryonic stem cell self-renewal. *Differentiation.* **75**, 299–307 (2007).
7. O. Gafni, L. Weinberger, A. A. Mansour, Y. S. Manor, E. Chomsky, D. Ben-Yosef, Y. Kalma, S. Viukov, I. Maza, A. Zviran, Y. Rais, Z. Shipony, Z. Mukamel, V. Krupalnik, M. Zerbib, S. Geula, I. Caspi, D. Schneir, T. Shwartz, S. Gilad, D. Amann-Zalcenstein, S. Benjamin, I. Amit, A. Tanay, R. Massarwa, N. Novershtern, J. H. Hanna, Derivation of novel human ground state naive pluripotent stem cells. *Nature* **504**, 282–286 (2013).
8. S. Kang, S. Dong, T.-L. Gu, A. Guo, M. S. Cohen, S. Lonial, H. J. Khoury, D. Fabbro, D. G. Gilliland, P. L. Bergsagel, J. Taunton, R. D. Polakiewicz, J. Chen, FGFR3

activates RSK2 to mediate hematopoietic transformation through tyrosine phosphorylation of RSK2 and activation of the MEK/ERK pathway. *Cancer Cell* **12**, 201–14 (2007).

9. V. Yadav, X. Zhang, J. Liu, S. Estrem, S. Li, X.-Q. Gong, S. Buchanan, J. R. Henry, J. J. Starling, S.-B. Peng, Reactivation of mitogen-activated protein kinase (MAPK) pathway by FGF receptor 3 (FGFR3)/Ras mediates resistance to vemurafenib in human B-RAF V600E mutant melanoma. *J. Biol. Chem.* **287**, 28087–98 (2012).
10. H. Ishikawa, N. Tsuyama, S. Liu, S. Abroun, F.-J. Li, K.-I. Otsuyama, X. Zheng, Z. Ma, Y. Maki, M. S. Iqbal, M. Obata, M. M. Kawano, Accelerated proliferation of myeloma cells by interleukin-6 cooperating with fibroblast growth factor receptor 3-mediated signals. *Oncogene* **24**, 6328–32 (2005).
11. Y. Zhen, V. Sørensen, Y. Jin, Z. Suo, A. Wiedłocha, Indirubin-3'-monoxime inhibits autophosphorylation of FGFR1 and stimulates ERK1/2 activity via p38 MAPK. *Oncogene* **26**, 6372–85 (2007).
12. P. Krejci, J. Prochazkova, J. Smutny, K. Chlebova, P. Lin, A. Aklian, V. Bryja, A. Kozubik, W. R. Wilcox, FGFR3 signaling induces a reversible senescence phenotype in chondrocytes similar to oncogene-induced premature senescence. *Bone* **47**, 102–10 (2010).
13. L. Dailey, E. Laplantine, R. Priore, C. Basilico, A network of transcriptional and signaling events is activated by FGF to induce chondrocyte growth arrest and differentiation. *J. Cell Biol.* **161**, 1053–66 (2003).
14. T. Matsushita, W. R. Wilcox, Y. Y. Chan, A. Kawanami, H. Bükülmez, G. Balmes, P. Krejci, P. B. Mekikian, K. Otani, I. Yamaura, M. L. Warman, D. Givol, S. Murakami, FGFR3 promotes synchondrosis closure and fusion of ossification centers through the MAPK pathway. *Hum. Mol. Genet.* **18**, 227–40 (2009).

15. S. Murakami, G. Balmes, S. McKinney, Z. Zhang, D. Givol, B. de Crombrugghe, Constitutive activation of MEK1 in chondrocytes causes Stat1-independent achondroplasia-like dwarfism and rescues the Fgfr3-deficient mouse phenotype. *Genes Dev.* **18**, 290–305 (2004).

16. H. Kouhara, Y. R. Hadari, T. Spivak-Kroizman, J. Schilling, D. Bar-Sagi, I. Lax, J. Schlessinger, A lipid-anchored Grb2-binding protein that links FGF-receptor activation to the Ras/MAPK signaling pathway. *Cell* **89**, 693–702 (1997).

17. Y. R. Hadari, H. Kouhara, I. Lax, J. Schlessinger, Binding of Shp2 tyrosine phosphatase to FRS2 is essential for fibroblast growth factor-induced PC12 cell differentiation. *Mol. Cell. Biol.* **18**, 3966–73 (1998).

18. M. Buchtova, V. Oralova, A. Aklian, J. Masek, I. Vesela, Z. Ouyang, T. Obadalova, Z. Konecna, T. Spoustova, T. Pospisilova, P. Matula, M. Varecha, L. Balek, I. Gudernova, I. Jelinkova, I. Duran, I. Cervenkova, S. Murakami, A. Kozubik, P. Dvorak, V. Bryja, P. Krejci, Fibroblast growth factor and canonical WNT/β-catenin signaling cooperate in suppression of chondrocyte differentiation in experimental models of FGFR signaling in cartilage. *Biochim. Biophys. Acta - Mol. Basis Dis.* **1852**, 839–850 (2015).

19. I. Gudernova, S. Foldynova-Trantirkova, B. E. El Ghannamova, B. Fafilek, M. Varecha, L. Balek, E. Hruba, L. Jonatova, I. Jelinkova, M. Kunova Bosakova, L. Trantirek, J. Mayer, P. Krejci, Y. Yen, S. Forman, R. Jove, M. Müller, R. Ezzeddine, A. Countouriotis, H. Kantarjian, T. Klinowska, G. Lamont, S. Lamont, N. Martin, H. McFarland, M. Mellor, J. Orme, D. Perkins, P. Perkins, G. Richmond, P. Smith, R. Ward, M. Waring, D. Whittaker, S. Wells, G. Wrigley, M. K. Bosakova, L. Trantirek, J. Mayer, P. Krejci, M. Bosakova Kunova, L. Trantirek, J. Mayer, P. Krejci, One reporter for in-cell activity profiling of majority of protein kinase oncogenes. *Elife* **6**,

117–120 (2017).

20. L. Balek, P. Nemec, P. Konik, M. Kunova Bosakova, M. Varecha, I. Gudernova, J. Medalova, D. Krakow, P. Krejci, Proteomic analyses of signalling complexes associated with receptor tyrosine kinase identify novel members of fibroblast growth factor receptor 3 interactome. *Cell. Signal.* **42**, 144–154 (2018).

21. P. L. Tavormina, R. Shiang, L. M. Thompson, Y.-Z. Zhu, D. J. Wilkin, R. S. Lachman, W. R. Wilcox, D. L. Rimoin, D. H. Cohn, J. J. Wasmuth, Thanatophoric dysplasia (types I and II) caused by distinct mutations in fibroblast growth factor receptor 3. *Nat. Genet.* **9**, 321–328 (1995).

22. N. Prasad, R. S. Topping, S. J. Decker, SH2-Containing Inositol 5'-Phosphatase SHIP2 Associates with the p130Cas Adapter Protein and Regulates Cellular Adhesion and Spreading. *Mol. Cell. Biol.* **21**, 1416–1428 (2001).

23. C. Erneux, S. Ghosh, A. R. Ramos, W. E. Edimo, New Functions of the Inositol Polyphosphate 5-Phosphatases in Cancer. *Curr. Pharm. Des.* **22**, 2309–14 (2016).

24. S. Ghosh, C. Huber, Q. Siour, S. B. Sousa, M. Wright, V. Cormier-Daire, C. Erneux, Fibroblasts derived from patients with opsismodysplasia display SHIP2-specific cell migration and adhesion defects. *Hum. Mutat.* **38**, 1731–1739 (2017).

25. T. Aikawa, G. V Segre, K. Lee, Fibroblast growth factor inhibits chondrocytic growth through induction of p21 and subsequent inactivation of cyclin E-Cdk2. *J. Biol. Chem.* **276**, 29347–52 (2001).

26. O. Rozenblatt-Rosen, E. Mosonego-Ornan, E. Sadot, L. Madar-Shapiro, Y. Sheinin, D. Ginsberg, A. Yayon, Induction of chondrocyte growth arrest by FGF: transcriptional and cytoskeletal alterations. *J. Cell Sci.* **115**, 553–62 (2002).

27. P. Krejci, B. Masri, L. Salazar, C. Farrington-Rock, H. Prats, L. M. Thompson, W. R. Wilcox, Bisindolylmaleimide I suppresses fibroblast growth factor-mediated activation

of Erk MAP kinase in chondrocytes by preventing Shp2 association with the Frs2 and Gab1 adaptor proteins. *J. Biol. Chem.* **282**, 2929–36 (2007).

28. B. Fafilek, M. Hampl, N. Ricankova, I. Vesela, L. Balek, M. Kunova Bosakova, I. Gudernova, M. Varecha, M. Buchtova, P. Krejci, Statins do not inhibit the FGFR signaling in chondrocytes. *Osteoarthr. Cartil.* **25**, 1522–1530 (2017).

29. H.-T. Lai, C.-M. Chiang, Bimolecular Fluorescence Complementation (BiFC) Assay for Direct Visualization of Protein-Protein Interaction in vivo. *Bio-protocol* **3** (available at http://www.ncbi.nlm.nih.gov/pubmed/27390756).

30. T. Wada, T. Sasaoka, M. Funaki, H. Hori, S. Murakami, M. Ishiki, T. Haruta, T. Asano, W. Ogawa, H. Ishihara, M. Kobayashi, Overexpression of SH2-Containing Inositol Phosphatase 2 Results in Negative Regulation of Insulin-Induced Metabolic Actions in 3T3-L1 Adipocytes via Its 5'-Phosphatase Catalytic Activity. *Mol. Cell. Biol.* **21**, 1633–1646 (2001).

31. Y. Ichihara, R. Fujimura, H. Tsuneki, T. Wada, K. Okamoto, H. Gouda, S. Hirono, K. Sugimoto, Y. Matsuya, T. Sasaoka, N. Toyooka, Rational design and synthesis of 4-substituted 2-pyridin-2-ylamides with inhibitory effects on SH2 domain-containing inositol 5′-phosphatase 2 (SHIP2). *Eur. J. Med. Chem.* **62**, 649–660 (2013).

32. M. Naïmi, N. Gautier, C. Chaussade, A. M. Valverde, D. Accili, E. Van Obberghen, Nuclear forkhead box O1 controls and integrates key signaling pathways in hepatocytes. *Endocrinology* **148**, 2424–34 (2007).

33. P. Krejci, V. Bryja, J. Pachernik, A. Hampl, R. Pogue, P. Mekikian, W. R. Wilcox, FGF2 inhibits proliferation and alters the cartilage-like phenotype of RCS cells. *Exp. Cell Res.* **297**, 152–164 (2004).

34. A. Raucci, E. Laplantine, A. Mansukhani, C. Basilico, Activation of the ERK1/2 and p38 mitogen-activated protein kinase pathways mediates fibroblast growth factor-

induced growth arrest of chondrocytes. *J. Biol. Chem.* **279**, 1747–56 (2004).

35. C. J. Marshall, Specificity of receptor tyrosine kinase signaling: transient versus sustained extracellular signal-regulated kinase activation. *Cell* **80**, 179–85 (1995).

36. M. A. Lemmon, J. Schlessinger, Cell Signaling by Receptor Tyrosine Kinases. *Cell* **141**, 1117–1134 (2010).

37. S. Yamada, T. Taketomi, A. Yoshimura, Model analysis of difference between EGF pathway and FGF pathway. *Biochem. Biophys. Res. Commun.* **314**, 1113–20 (2004).

38. V. Knights, S. J. Cook, De-regulated FGF receptors as therapeutic targets in cancer. *Pharmacol. Ther.* **125**, 105–17 (2010).

39. I. Mellman, Y. Yarden, Endocytosis and cancer. *Cold Spring Harb. Perspect. Biol.* **5**, a016949 (2013).

40. B. Nadratowska-Wesolowska, E. M. Haugsten, M. Zakrzewska, P. Jakimowicz, Y. Zhen, D. Pajdzik, J. Wesche, A. Wiedlocha, RSK2 regulates endocytosis of FGF receptor 1 by phosphorylation on serine 789. *Oncogene* **33**, 4823–36 (2014).

41. M. Chesi, E. Nardini, L. A. Brents, E. Schröck, T. Ried, W. M. Kuehl, P. L. Bergsagel, Frequent translocation t(4;14)(p16.3;q32.3) in multiple myeloma is associated with increased expression and activating mutations of fibroblast growth factor receptor 3. *Nat. Genet.* **16**, 260–4 (1997).

42. L. Xie, X. Su, L. Zhang, X. Yin, L. Tang, X. Zhang, Y. Xu, Z. Gao, K. Liu, M. Zhou, B. Gao, D. Shen, L. Zhang, J. Ji, P. R. Gavine, J. Zhang, E. Kilgour, X. Zhang, Q. Ji, FGFR2 gene amplification in gastric cancer predicts sensitivity to the selective FGFR inhibitor AZD4547. *Clin. Cancer Res.* **19**, 2572–83 (2013).

43. J. Weiss, M. L. Sos, D. Seidel, M. Peifer, T. Zander, J. M. Heuckmann, R. T. Ullrich, R. Menon, S. Maier, A. Soltermann, H. Moch, P. Wagener, F. Fischer, S. Heynck, M. Koker, J. Schöttle, F. Leenders, F. Gabler, I. Dabow, S. Querings, L. C. Heukamp, H.

Balke-Want, S. Ansén, D. Rauh, I. Baessmann, J. Altmüller, Z. Wainer, M. Conron, G. Wright, P. Russell, B. Solomon, E. Brambilla, C. Brambilla, P. Lorimier, S. Sollberg, O. T. Brustugun, W. Engel-Riedel, C. Ludwig, I. Petersen, J. Sänger, J. Clement, H. Groen, W. Timens, H. Sietsma, E. Thunnissen, E. Smit, D. Heideman, F. Cappuzzo, C. Ligorio, S. Damiani, M. Hallek, R. Beroukhim, W. Pao, B. Klebl, M. Baumann, R. Buettner, K. Ernestus, E. Stoelben, J. Wolf, P. Nürnberg, S. Perner, R. K. Thomas, Frequent and focal FGFR1 amplification associates with therapeutically tractable FGFR1 dependency in squamous cell lung cancer. *Sci. Transl. Med.* **2** (2010), doi:10.1126/scitranslmed.3001451.

44. A. Wong, B. Lamothe, A. Lee, J. Schlessinger, I. Lax, A. Li, FRS2 alpha attenuates FGF receptor signaling by Grb2-mediated recruitment of the ubiquitin ligase Cbl. *Proc. Natl. Acad. Sci. U. S. A.* **99**, 6684–9 (2002).

45. I. Lax, A. Wong, B. Lamothe, A. Lee, A. Frost, J. Hawes, J. Schlessinger, The docking protein FRS2alpha controls a MAP kinase-mediated negative feedback mechanism for signaling by FGF receptors. *Mol. Cell* **10**, 709–19 (2002).

46. N. Gotoh, Regulation of growth factor signaling by FRS2 family docking/scaffold adaptor proteins. *Cancer Sci.* **99**, 1319–25 (2008).

47. M. Muda, U. Boschert, R. Dickinson, J. C. Martinou, I. Martinou, M. Camps, W. Schlegel, S. Arkinstall, MKP-3, a novel cytosolic protein-tyrosine phosphatase that exemplifies a new class of mitogen-activated protein kinase phosphatase. *J. Biol. Chem.* **271**, 4319–26 (1996).

48. A. Sasaki, T. Taketomi, R. Kato, K. Saeki, A. Nonami, M. Sasaki, M. Kuriyama, N. Saito, M. Shibuya, A. Yoshimura, Mammalian Sprouty4 suppresses Ras-independent ERK activation by binding to Raf1. *Nat. Cell Biol.* **5**, 427–432 (2003).

49. N. E. Kremer, G. D'Arcangelo, S. M. Thomas, M. DeMarco, J. S. Brugge, S.

Halegoua, Signal transduction by nerve growth factor and fibroblast growth factor in PC12 cells requires a sequence of src and ras actions. *J. Cell Biol.* **115**, 809–19 (1991).

50. J. M. Rodier, A. M. Vallés, M. Denoyelle, J. P. Thiery, B. Boyer, pp60c-src is a positive regulator of growth factor-induced cell scattering in a rat bladder carcinoma cell line. *J. Cell Biol.* **131**, 761–73 (1995).

51. A. P. Belsches, M. D. Haskell, S. J. Parsons, Role of c-Src tyrosine kinase in EGF-induced mitogenesis. *Front. Biosci.* **2**, d501-18 (1997).

52. J. Liu, C. Huang, X. Zhan, Src is required for cell migration and shape changes induced by fibroblast growth factor 1. *Oncogene* **18**, 6700–6 (1999).

53. P. Klint, S. Kanda, Y. Kloog, L. Claesson-Welsh, Contribution of Src and Ras pathways in FGF-2 induced endothelial cell differentiation. *Oncogene* **18**, 3354–64 (1999).

54. F. Debiais, J. Lemonnier, E. Hay, P. Delannoy, J. Caverzasio, P. J. Marie, Fibroblast growth factor-2 (FGF-2) increases N-cadherin expression through protein kinase C and Src-kinase pathways in human calvaria osteoblasts. *J. Cell. Biochem.* **81**, 68–81 (2001).

55. D. M. Kilkenny, J. V Rocheleau, J. Price, M. B. Reich, G. G. Miller, c-Src regulation of fibroblast growth factor-induced proliferation in murine embryonic fibroblasts. *J. Biol. Chem.* **278**, 17448–54 (2003).

56. S. Knuchel, P. Anderle, P. Werfelli, E. Diamantis, C. Rüegg, Fibroblast surface-associated FGF-2 promotes contact-dependent colorectal cancer cell migration and invasion through FGFR-SRC signaling and integrin αvβ5-mediated adhesion. *Oncotarget* **6**, 14300–17 (2015).

57. X. Zhan, C. Plourde, X. Hu, R. Friesel, T. Maciag, Association of fibroblast growth factor receptor-1 with c-Src correlates with association between c-Src and cortactin. *J.*

Biol. Chem. **269**, 20221–4 (1994).

58. J. Hama, H. Xu, M. Goldfarb, D. C. Weinstein, SNT-1/FRS2alpha physically interacts with Laloo and mediates mesoderm induction by fibroblast growth factor. *Mech. Dev.* **109**, 195–204 (2001).

59. P. Zhang, J. S. S. Greendorfer, J. Jiao, S. C. C. Kelpke, J. A. A. Thompson, Alternatively spliced FGFR-1 isoforms differentially modulate endothelial cell activation of c-YES. *Arch. Biochem. Biophys.* **450**, 50–62 (2006).

60. T. Shono, H. Kanetake, S. Kanda, The role of mitogen-activated protein kinase activation within focal adhesions in chemotaxis toward FGF-2 by murine brain capillary endothelial cells. *Exp. Cell Res.* **264**, 275–83 (2001).

61. S. Clément, U. Krause, F. Desmedt, J.-F. Tanti, J. Behrends, X. Pesesse, T. Sasaki, J. Penninger, M. Doherty, W. Malaisse, J. E. Dumont, Y. Le Marchand-Brustel, C. Erneux, L. Hue, S. Schurmans, The lipid phosphatase SHIP2 controls insulin sensitivity. *Nature* **409**, 92–97 (2001).

62. M. W. Sleeman, K. E. Wortley, K.-M. V Lai, L. C. Gowen, J. Kintner, W. O. Kline, K. Garcia, T. N. Stitt, G. D. Yancopoulos, S. J. Wiegand, D. J. Glass, Absence of the lipid phosphatase SHIP2 confers resistance to dietary obesity. *Nat. Med.* **11**, 199–205 (2005).

63. B. Li, D. Krakow, D. A. Nickerson, M. J. Bamshad, Y. University of Washington Center for Mendelian Genomics, Y. Chang, R. S. Lachman, A. Yilmaz, H. Kayserili, D. H. Cohn, Opsismodysplasia resulting from an insertion mutation in the SH2 domain, which destabilizes INPPL1. *Am. J. Med. Genet. A* **164A**, 2407–11 (2014).

64. J. E. Below, D. L. Earl, K. M. Shively, M. J. McMillin, J. D. Smith, E. H. Turner, M. J. Stephan, L. I. Al-Gazali, J. L. Hertecant, D. Chitayat, S. Unger, D. H. Cohn, D. Krakow, J. M. Swanson, E. M. Faustman, J. Shendure, D. A. Nickerson, M. J.

Bamshad, University of Washington Center for Mendelian Genomics, Whole-genome analysis reveals that mutations in inositol polyphosphate phosphatase-like 1 cause opsismodysplasia. *Am. J. Hum. Genet.* **92**, 137–43 (2013).

65. C. Feist, P. Holden, J. Fitzgerald, Novel compound heterozygous mutations in inositol polyphosphate phosphatase-like 1 in a family with severe opsismodysplasia. *Clin. Dysmorphol.* **25**, 152–5 (2016).

66. H. Lee, L. Nevarez, R. S. Lachman, W. R. Wilcox, D. Krakow, D. H. Cohn, University of Washington Center for Mendelian Genomics, A second locus for Schneckenbecken dysplasia identified by a mutation in the gene encoding inositol polyphosphate phosphatase-like 1 (INPPL1). *Am. J. Med. Genet. A* **167A**, 2470–3 (2015).

67. V. Cormier-Daire, A. L. Delezoide, N. Philip, P. Marcorelles, K. Casas, Y. Hillion, L. Faivre, D. L. Rimoin, A. Munnich, P. Maroteaux, M. Le Merrer, Clinical, radiological, and chondro-osseous findings in opsismodysplasia: survey of a series of 12 unreported cases. *J. Med. Genet.* **40**, 195–200 (2003).

68. C. Fyffe, M. Falasca, 3-Phosphoinositide-dependent protein kinase-1 as an emerging target in the management of breast cancer. *Cancer Manag. Res.* **5**, 271–80 (2013).

69. C. Huber, E. A. Faqeih, D. Bartholdi, C. Bole-Feysot, Z. Borochowitz, D. P. Cavalcanti, A. Frigo, P. Nitschke, J. Roume, H. G. Santos, S. A. Shalev, A. Superti-Furga, A.-L. Delezoide, M. Le Merrer, A. Munnich, V. Cormier-Daire, Exome sequencing identifies INPPL1 mutations as a cause of opsismodysplasia. *Am. J. Hum. Genet.* **92**, 144–9 (2013).

70. A. Fradet, J. Fitzgerald, INPPL1 gene mutations in opsismodysplasia. *J. Hum. Genet.* **62**, 135–140 (2017).

71. A. Kasprzak, W. Kwasniewski, A. Adamek, A. Gozdzicka-Jozefiak, Insulin-like growth factor (IGF) axis in cancerogenesis. *Mutat. Res. Mutat. Res.* **772**, 78–104

(2017).

72. J. Baker, J. P. Liu, E. J. Robertson, A. Efstratiadis, Role of insulin-like growth factors in embryonic and postnatal growth. *Cell* **75**, 73–82 (1993).

73. Y. Wang, S. Nishida, T. Sakata, H. Z. Elalieh, W. Chang, B. P. Halloran, S. B. Doty, D. D. Bikle, Insulin-like growth factor-I is essential for embryonic bone development. *Endocrinology* **147**, 4753–61 (2006).

74. Y. Wang, Z. Cheng, H. Z. Elalieh, E. Nakamura, M.-T. Nguyen, S. Mackem, T. L. Clemens, D. D. Bikle, W. Chang, IGF-1R signaling in chondrocytes modulates growth plate development by interacting with the PTHrP/Ihh pathway. *J. Bone Miner. Res.* **26**, 1437–46 (2011).

75. K. Mukhopadhyay, V. Lefebvre, G. Zhou, S. Garofalo, J. H. Kimura, B. de Crombrugghe, Use of a new rat chondrosarcoma cell line to delineate a 119-base pair chondrocyte-specific enhancer element and to define active promoter segments in the mouse pro-alpha 1(II) collagen gene. *J. Biol. Chem.* **270**, 27711–9 (1995).

76. E. M. Haugsten, A. Brech, K. Liestøl, J. C. Norman, J. Wesche, Photoactivation Approaches Reveal a Role for Rab11 in FGFR4 Recycling and Signalling. *Traffic* **15**, 665–683 (2014).

77. M. Kostas, E. M. Haugsten, Y. Zhen, V. Sorensen, P. Szybowska, E. Fiorito, S. Lorenz, G. A. de Souza, A. Wiedlocha, J. Wesche, *Mol. Cell. Proteomics*, in press.

78. W. Elong Edimo, S. Ghosh, R. Derua, V. Janssens, E. Waelkens, J.-M. Vanderwinden, P. Robe, C. Erneux, SHIP2 controls plasma membrane PI(4,5)P2 thereby participating in the control of cell migration in 1321 N1 glioblastoma cells. *J. Cell Sci.* **129**, 1101–14 (2016).

79. I. Gudernova, S. Foldynova-Trantirkova, B. El Ghannamova, B. Fafilek, M. Varecha, L. Balek, E. Hruba, L. Jonatova, I. Jelinkova, M. K. Bosakova, L. Trantirek, J. Mayer,

P. Krejci, One reporter for in-cell activity profiling of majority of protein kinase oncogenes. *Elife* **6** (2017).

80. I. Gudernova, I. Vesela, L. Balek, M. Buchtova, H. Dosedelova, M. Kunova, J. Pivnicka, I. Jelinkova, L. Roubalova, A. Kozubik, P. Krejci, Multikinase activity of fibroblast growth factor receptor (FGFR) inhibitors SU5402, PD173074, AZD1480, AZD4547 and BGJ398 compromises the use of small chemicals targeting FGFR catalytic activity for therapy of short-stature syndromes. *Hum. Mol. Genet.* **25**, 9–23 (2016).

81. F. A. Ran, P. D. Hsu, J. Wright, V. Agarwala, D. A. Scott, F. Zhang, Genome engineering using the CRISPR-Cas9 system. *Nat. Protoc.* **8**, 2281–2308 (2013).

82. T. G. Montague, J. M. Cruz, J. A. Gagnon, G. M. Church, E. Valen, CHOPCHOP: a CRISPR/Cas9 and TALEN web tool for genome editing. *Nucleic Acids Res.* **42**, W401–W407 (2014).

Acknowledgements

We thank Pavel Nemec for excellent technical assistance, Vladimir Korinek for GReP plasmid, and Antoni Wiedlocha for helpful discussions. Supported by Ministry of Education, Youth and Sports of the Czech Republic (KONTAKT II LH15231); Agency for Healthcare Research of the Czech Republic (15-33232A, 15-34405A); Czech Science Foundation (GA17-09525S); National Program of Sustainability II (MEYS CR: LQ1605 and CEITEC 2020 (LQ1601)). This work was partially supported by the Research Council of Norway through its Centers of Excellence funding scheme, project number 262652. E.M.H has a Career fellowship (project 6842225) from the Norwegian Cancer Society. MKB was supported by junior researcher funds from the Faculty of Medicine, Masaryk University. JTZ was supported by Kohn fellowship at Masaryk University and National Institute of Arthritis and Musculoskeletal and Skin Diseases

of the National Institutes of Health (1F31AR066487). DK is supported by NIH grants R01-AR066124 and R01-AR062651. The content is solely the responsibility of the authors and does not necessarily represent the official views of the National Institutes of Health. CE is supported by grants from the Université Libre de Bruxelles and of the Fonds de la Recherche Scientifique Médicale (J.0078.18). SG is supported by Hoguet, Fonds Lekime-Ropsy and Télévie fellowships.

Figure Legends

Figure 1 FGFRs interact with SHIP2 and phosphorylate SHIP2 in cells

(A) 293T cells were transfected with V5-tagged wildtype (WT) FGFR3 or FGFR3-K650M together with FLAG-tagged SHIP2 and subjected to V5 or FLAG immunoprecipitation (IP) 24 hours later. Note the SHIP2 phosphorylation in cells transfected with activating K650M FGFR3 mutant (SH. SHIP2, FG. FGFR3). Immunoblot with SHIP2 antibody shows both endogenous and transgenic SHIP2. (B) Cell-free kinase assay utilizing recombinant FGFR3 as a kinase and recombinant SHIP2 as a substrate demonstrate SHIP2 phosphorylation by FGFR3. Sample with ATP omitted serves as negative control. 4G10, pan-specific phosphotyrosine antibody. (C) Cell-free kinase assay demonstrating no effect of recombinant SHIP2 on FGFR3 activity determined as the level of FGFR3 autophosphorylation in samples where FGFR3 was inhibited by addition of FGFR inhibitor (SU5402) for 20 minutes. Data are representative for three independent experiments. (D) Cell-free colorimetric SHIP2 phosphatase activity assay determining the SHIP2-mediated hydrolysis of phosphoinositide PtdIns(3,4,5)P3 (PIP3) to PtdIns(3,4)P2 (PIP2), carried out as described in Material and Methods. Recombinant active SHIP2 and FGFR3 were added to reaction buffer. Samples with omitted ATP serve as negative controls for FGFR3 activity. Note that addition of FGFR3 does not significantly alter SHIP2 catalytic activity (n.s., Welch's t-test). Columns show compilation of three independent

experiments (n) with indicated SD. For each of them the values were calculated as averages from two technical duplicates, each measured three times.

Figure 2 SHIP2 interacts with FGFR3 via SH2 and SAM domains

(A) Schematic representation of generated truncated SHIP2 constructs. V5 epitope was added for immunoprecipitation (IP). SH2, SRC-homology domain 2; PR, proline-rich domain; PS, inositol phosphatase; SAM, sterile alpha motif. (B-E) SHIP2 variants were expressed with wildtype FGFR3 in 293T cells, immunoprecipitated and analyzed by western blotting (WB). Actin serves as a loading control. Input, total cell lysates used for IP. Note the normal association of SHIP2 lacking PS or PR1 domain with FGFR3 (B, C), compared to diminished association of variants lacking SH2 domain or N-terminal SAM domain (D, E, arrows). (F) No co-immunoprecipitation of SHIP2 with catalytically-inactive K508M mutant of FGFR3 was found. Data are representative for three independent experiments.

Figure 3 SHIP2 interacts with FGFR1

(A) 293T cells were transfected with V5-tagged wildtype FGFR1, FGFR2 and FGFR4 together with FLAG-tagged SHIP2 and subjected to FLAG immunoprecipitation (IP) 24 hours later. Note that FGFR1 and FGFR4 but not FGFR2 interact with SHIP2. (B-E) U2OS cells stably expressing FGFR1-GFP were treated with 25 ng/ml FGF2 for 15 minutes, fixed and subjected to proximity ligation assay (PLA) using antibodies detecting SHIP2 and GFP (B, C), or SHIP2 and FGFR1 (D, E). U2OS cells stably expressing FGFR1-BirA-HA or FGFR4-GFP were used as negative controls in A, C and B, D, respectively. Data are mean±SEM. Statistical significance was determined by Welch’s t-test with Bonferroni's correction of p values (n.s. $p>0.05$, ***$p<0.001$). Scale bar, 20 µm; n, number of independent experiments.

Figure 4 FGF signaling targets SHIP2 to focal adhesions

(A) Phosphorylation of endogenous SHIP2 triggered by activation of FGF signaling in RCS cells treated with FGF2 for indicated times. (B) FGF2 triggers translocation of phosphorylated (p) SHIP2$^{Y986/7}$ to the peripheral focal adhesions (arrows), where it co-localizes with vinculin (C; arrows). (D) Similar effect is observed on p130CAS phosphorylated at Tyr^{410} upon FGF2 treatment (pp130CAS). Bar, 25 μm. (E) Higher magnification of squares selected in C and D. (F) Genotype and corresponding SHIP2 protein amounts in four SHIP2^{Crispr} RCS cell lines, compared to wildtype RCS cells. (G) To measure migration, wildtype RCS cells and SHIP2^{Crispr} cell lines were starved overnight, treated with 10% FCS or FGF2 [25 ng/ml] for 8 hours, and individually tracked for 15 hours. Data are mean ± SEM. Statistical significance was determined by Welch's t-test with Bonferroni's correction of p values, ***p<0.0001. Data are representative for three independent experiments. Christophe is G representative for 3 experiments or compilation of three independent experiments? Please check

Figure 5 Loss of SHIP2 rescues cell phenotypes regulated by FGF signaling

(A) A rescue of the FGF2-mediated inhibition of RCS proliferation (FGF2 treatment for 96 hours) in four different SHIP2^{Crispr} cell lines, determined by crystal violet staining. Data represent averages from 8 wells with indicated standard deviation. Statistically significant differences are highlighted (***p<0.001, Welch's t-test). (B, C) No rescue is observed in three randomly selected RCS clones with normal SHIP2 amount. (D, E) The rescue of FGF2-mediated loss of RCS cartilaginous extracellular matrix (ECM) in SHIP2^{Crispr} cells, determined by collagen 2 western blot for collagen ECM (D; treatment with 25ng/ml FGF2 for 48 hours), and alcian blue staining for sulfated proteoglycan ECM (FGF2 treatment for 72 hours) (E; fig. S1). (D) Poor FGF2-mediated induction of senescence marker caveolin 1 in SHIP2^{Crispr} cells is also shown. (F) Evidence for spreading in cells treated with FGF2 for 72 hours, due to the

formation of actin stress fibers, visualized by phalloidin staining (G). This phenotype is not rescued SHIP2^{Crispr}. Scale bars 20 μm. Data are representative for three independent experiments.

Figure 6 Loss of SHIP2 impairs FGFR-ERK signaling

(A) Wildtype (WT) and SHIP2^{Crispr} (Ship2$^{a+/-}$) RCS cells were treated with FGF2 (20 ng/ml) for indicated times and analyzed for phosphorylated (p) forms of FRS2, GAB1, AKT and ERK by western blot. Note the impaired FGF2-mediated phosphorylation of FRS2 and GAB1 adapters with corresponding under-phosphorylation of ERK. Actin and total level of given protein serve as loading controls. Additional analyses carried out in other SHIP2^{Crispr} cell lines are shown at figure S3, A to C. Data are representative for at least three independent experiments. (B) Quantification of SHIP2 protein in wildtype RCS cells using western blot of RCS lysates and serial dilutions of recombinant (rec) SHIP2. Densitometry was used to quantify the band intensities and to obtain information on cellular SHIP2 numbers (287,546±37,305 molecules per single cell, mean±SEM; n=9). (C) Two SHIP2^{Crispr} cell lines were microinjected with amount of recombinant SHIP2 (recSHIP2) of approximately 1/10th (~25,000 molecules/cell) of the endogenous SHIP2, together with dTomato transcriptional reporter to ERK activity (pKrox24(MapErk)^{dTomato}). Cells were treated with FGF2 and the dsTomato expression was analyzed 24 hours later and plotted. (E) RecSHIP2 rescued the FGF ability to activate of ERK pathway in SHIP2^{Crispr} cells (Student´s t-test, ***$p<0.001$, **$p<0.01$). Scale bars, 20 μm (C) and 200 μm (E); Ph2, phase contrast. (F) Wildtype and Ship2$^{a+/-}$ RCS cells were treated with FGF2 for indicated times, FRS2 was immunoprecipitated (IP) and its immunocomplexes were analyzed for PTPN11 presence by western blot. Note the impaired FRS2-PTPN11 association in FGF2-treated SHIP2^{Crispr} cells.

Figure 7 SHIP2 promotes association of SRC-family kinases with FGFR3

(A) 293T cells were transfected with FLAG-tagged wildtype (WT) FGFR3 or K650E activating mutant of FGFR3 together with SRC-family kinase LCK. FGFR3 was immunoprecipitated (IP) 24 hours later and immunocomplexes were analyzed for FGFR3 and LCK by western blot. Note the FGFR3 association with LCK. Additional experiments show association of other SRC kinases such as FYN, LYN, FGR and BLK with FGFR3 (fig. S5). (B) RCS cells were transfected with vectors expressing FGFR3-Venus2 (V2) and Lyn-Venus1 (V1), fixed 24 hours later, counterstained visualize Venus expression (ICC), and the percentage of transfected cells complementing Venus was calculated and plotted (C). (mean±SEM). Note the Venus fluorescence at the cell membrane, in the cytosol and Golgi. Scale bar, 10 μm. (D) RCS cells and (E) 293T cells were treated with 20 ng/ml of FGF2 (1.5 hour) alone or in the presence of SRC inhibitors AZM475271 and A419259 and analyzed for FRS2 and ERK phosphorylation (p). Total FRS2 and ERK amounts serve as loading controls. Note the inhibition of FRS2 and ERK phosphorylation by SRC inhibitors. (F) Expression of wildtype FGFR3 in RCS cells causes its activation evidenced by western blot for autophosphorylated (p) FGFR3. This phosphorylation is sensitive to inhibition of FGFR3 catalytic activity by treatment with FGFR inhibitor AZD4547 (AZD.). (G) Representative images of FGFR3 interaction with SRC kinase YES (tagged with YFP) in RCS cells, probed by proximity ligation assay (PLA). Scale bar, 10 μM. Note the PLA dots at the cell membrane, illuminating the site of FGFR3-YES interaction. (H) Compilation of three (n) independent PLA experiments demonstrating lesser extent of FGFR3-YES interaction in two $SHIP2^{Crispr}$ cell lines ($Ship2^{c-/-}$, $Ship2^{a+/-}$), compared to wildtype RCS cells. Transfections containing empty vector and vector expressing YFP serve as negative control for PLA assay. Data represent averages with indicated SEM (*$p<0.05$, ***$p<0.001$; Welch's t-test with Bonferroni's correction of p values).

Figure 8 Inositol phosphatase activity of SHIP2 is not necessary for its association with FGFR signaling complex and for FGF-mediated ERK activation

(A-C) Co-immunoprecipitation (IP) analyses of SHIP2 and its partners expressed in 293T cells demonstrate that catalytically inactive SHIP2, due to P686A/D690A/R691A substitutions (SHIP2-PD) or deletion of an entire inositol phosphatase domain (SHIP2-ΔPS), associates normally with FRS2 or with SRC kinases LCK and LYN. Non-transfected cells or those transfected with GFP serve as negative IP controls. Actin serves as loading control. (D) RCS cells were treated with inhibitor of SHIP2 phosphatase activity AS1949490 (AS19.) and FGF2 (40 ng/ml) for indicated times and analyzed for phosphorylated (p) forms of indicated proteins by western blot. Actin and total level of given protein serve as loading controls. Note the AS1949490-mediated increase in phosphorylation of AKT and its substrate FoxO1 in cells treated with FGF2 for 6-10 hours (arrows). The activating phosphorylation of ERK is also increased. (E) RCS cells were transfected with wildtype SHIP2 or SHIP2-ΔPS together with firefly luciferase pKrox24 reporter plasmid and *Renilla* luciferase pTK-RL control plasmid. Cells were treated with FGF2 for 24 hours and the FGF2-mediated pKrox24 transactivation was determined by dual-luciferase assay. Note the enhanced response to FGF2 in cells transfected with SHIP2, compared to cells transfected with empty plasmid. This phenotype is more pronounced in cells transfected with catalytically inactive SHIP2. Data are compilation of three independent experiments, four biological and two technical replicates were analyzed in each experiment. Bars are averages with indicated SD (**$p<0.01$, ***$p<0.001$; Welch's t-test with Bonferroni's correction of p values). (F) A role of SHIP2 in canonical FGFR-ERK signaling. Activated FGFRs phosphorylate SHIP2 and recruit SHIP2 to the FGFR signaling complex at the cell membrane. SHIP2 knock-out by CRISPR/Cas9 technology effectively converts FGF-mediated *sustained* ERK activation into the *transient* one and rescues the cell phenotypes induced by sustained FGFR-ERK signaling (premature senescence, ECM

degradation, growth arrest). This is due to under-phosphorylation of GAB1 and FRS2 adapters in SHIP2^{Crispr} cells, resulting in diminished recruitment of PTPN11-SOS1 complexes which activate of RAS-ERK signaling module. SHIP2 associates with SRC-family kinases and bring SRC kinases to the FGFR signaling complexes where they assist FGFR-mediated ERK activation by increasing adapter phosphorylation.

Figure 1

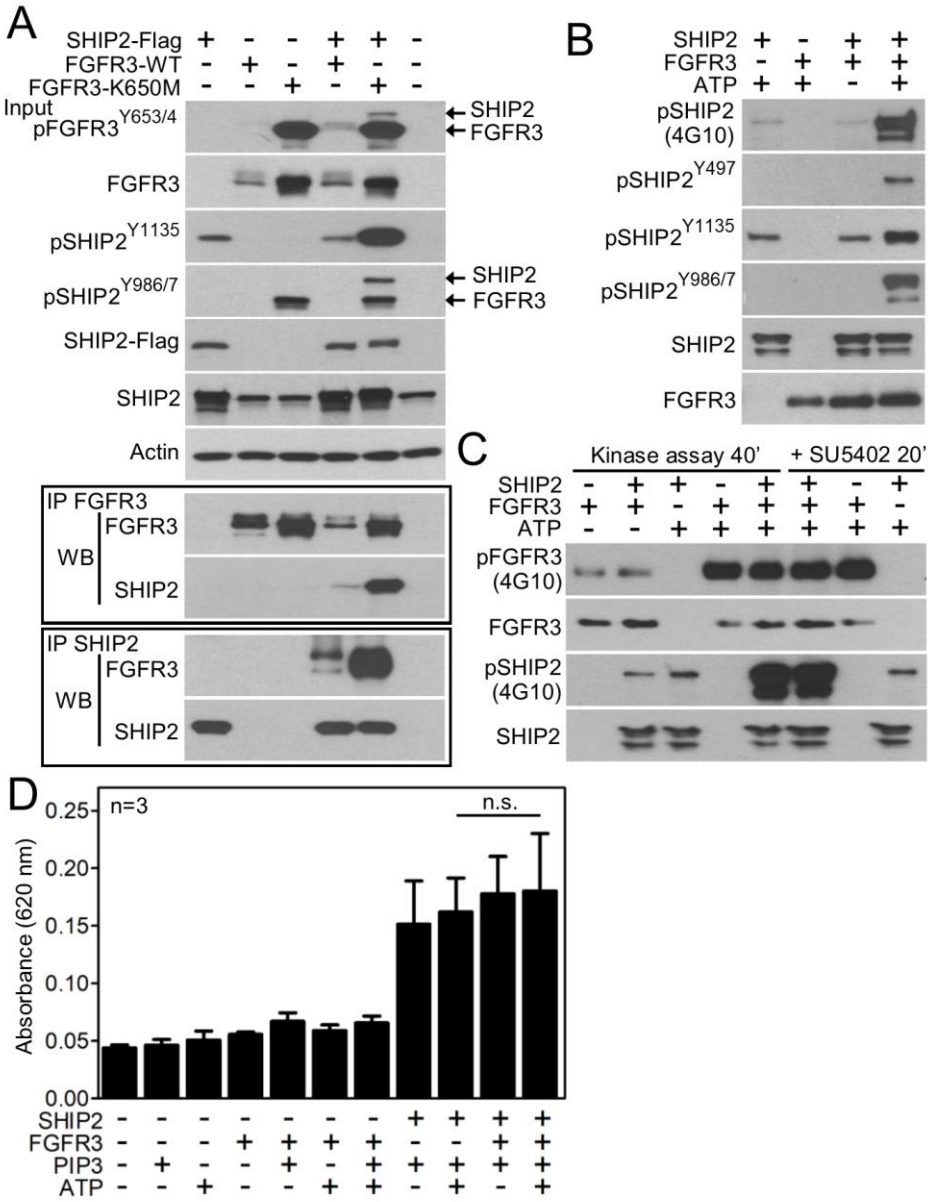
A
SHIP2-Flag
FGFR3-WT
FGFR3-K650M
Input
pFGFR3Y653/4
FGFR3
pSHIP2Y1135
pSHIP2Y986/7
SHIP2-Flag
SHIP2
Actin
SHIP2
FGFR3
IP FGFR3
WB
FGFR3
SHIP2
IP SHIP2
WB
FGFR3
SHIP2
B
SHIP2
FGFR3
ATP
pSHIP2 (4G10)
pSHIP2Y497
pSHIP2Y1135
pSHIP2Y986/7
SHIP2
FGFR3
C
Kinase assay 40'
+ SU5402 20'
SHIP2
FGFR3
ATP
pFGFR3 (4G10)
FGFR3
pSHIP2 (4G10)
SHIP2
D
n=3
n.s.
Absorbance (620 nm)
0.25
0.20
0.15
0.10
0.05
0.00
SHIP2
FGFR3
PIP3
ATP

Figure 2

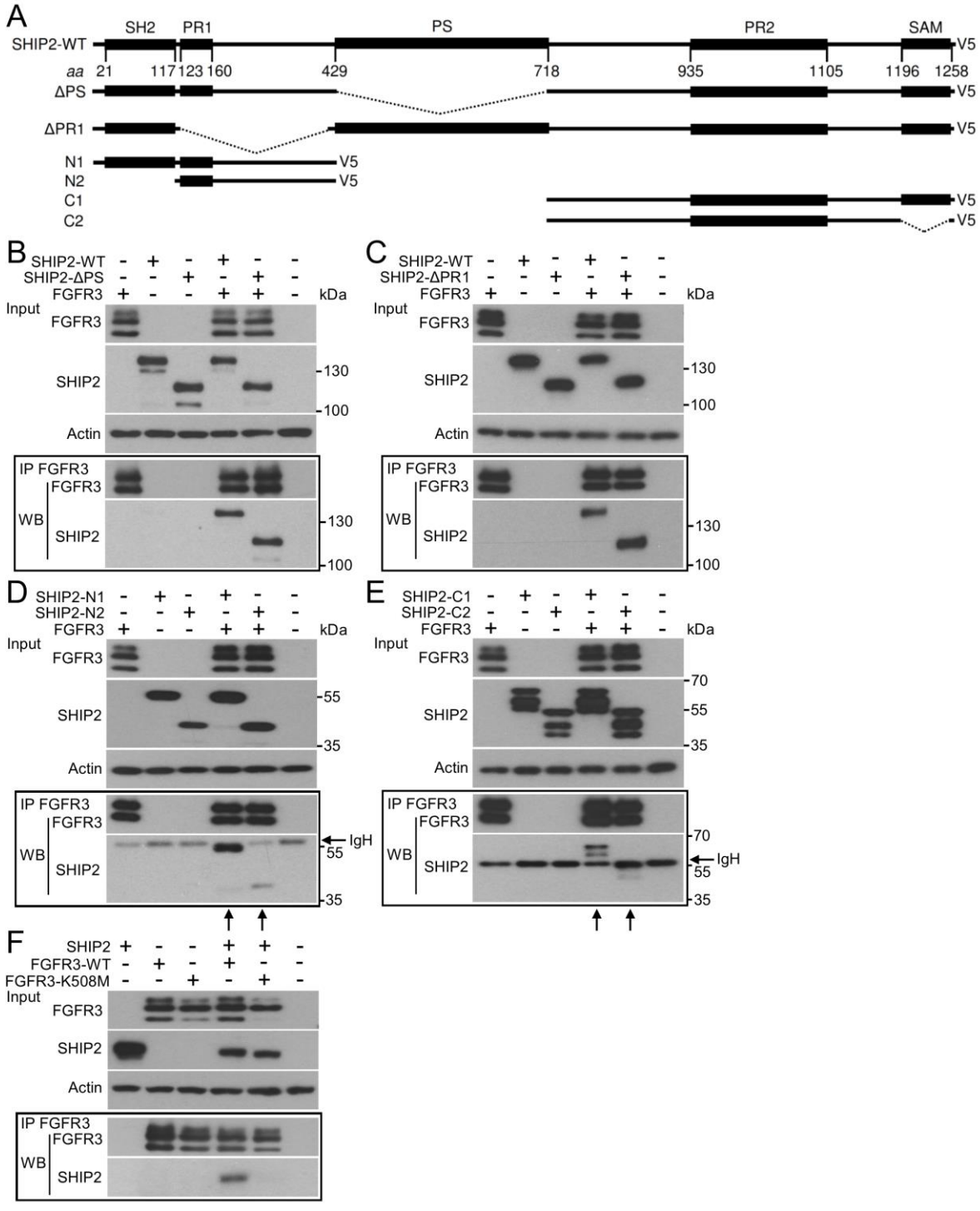
A
SH2
PR1
PS
PR2
SAM
SHIP2-WT
V5
aa 21 117 123 160 429 718 935 1105 1196 1258
ΔPS
ΔPR1
N1
N2
C1
C2
B
SHIP2-WT
SHIP2-ΔPS
FGFR3
kDa
Input
FGFR3
SHIP2
Actin
130
100
IP FGFR3
WB
C
SHIP2-ΔPR1
D
SHIP2-N1
SHIP2-N2
55
35
IgH
E
SHIP2-C1
SHIP2-C2
70
F
SHIP2
FGFR3-WT
FGFR3-K508M

Figure 3

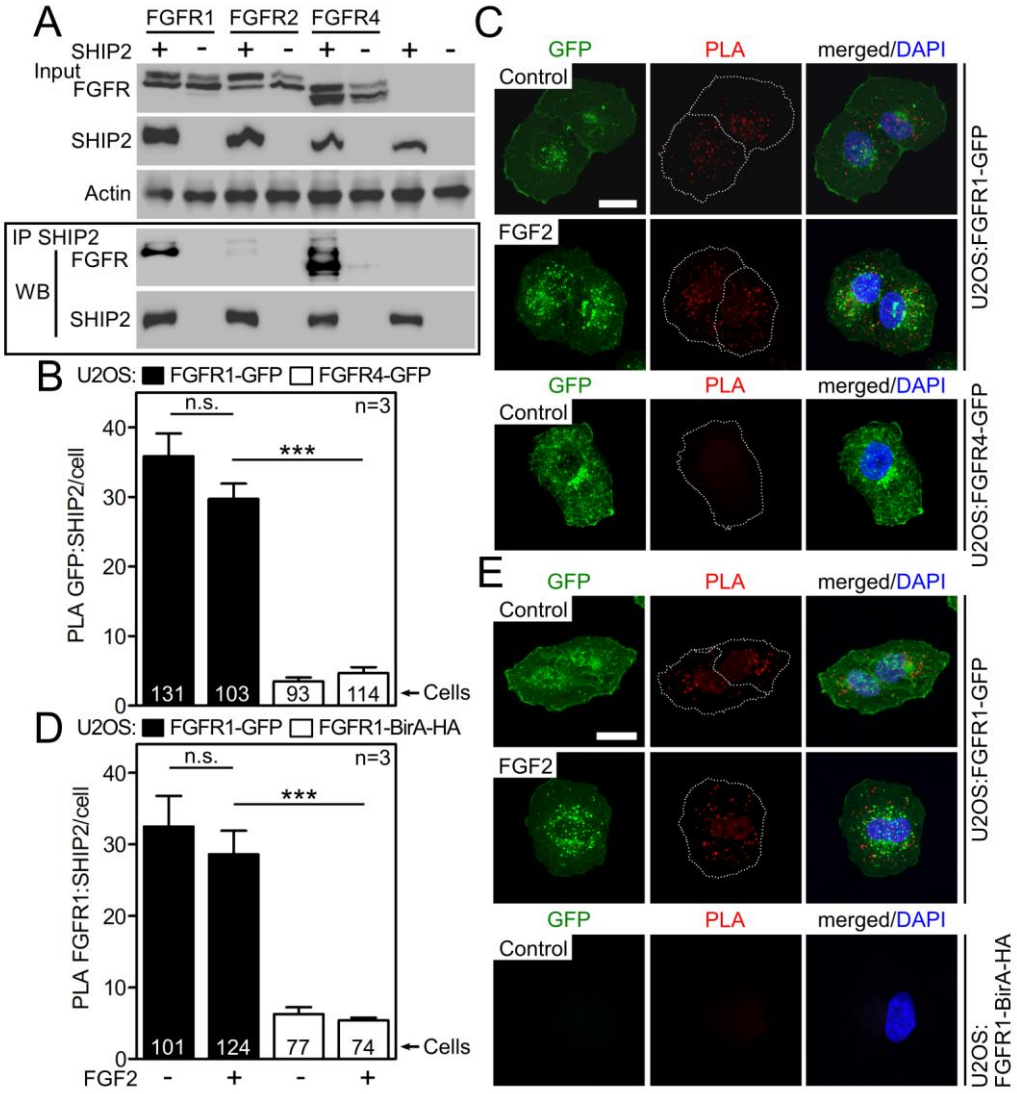
A
FGFR1
FGFR2
FGFR4
SHIP2 + - + - + - + -
Input
FGFR
SHIP2
Actin
IP SHIP2
WB
FGFR
SHIP2
B
U2OS: FGFR1-GFP FGFR4-GFP
n.s.
n=3
***
PLA GFP:SHIP2/cell
131
103
93
114
Cells
D
U2OS: FGFR1-GFP FGFR1-BirA-HA
n.s.
n=3
***
PLA FGFR1:SHIP2/cell
101
124
77
74
Cells
FGF2 - + - +
C
GFP
PLA
merged/DAPI
Control
FGF2
U2OS:FGFR1-GFP
U2OS:FGFR4-GFP
E
GFP
PLA
merged/DAPI
Control
FGF2
U2OS:FGFR1-GFP
U2OS: FGFR1-BirA-HA

Figure 4

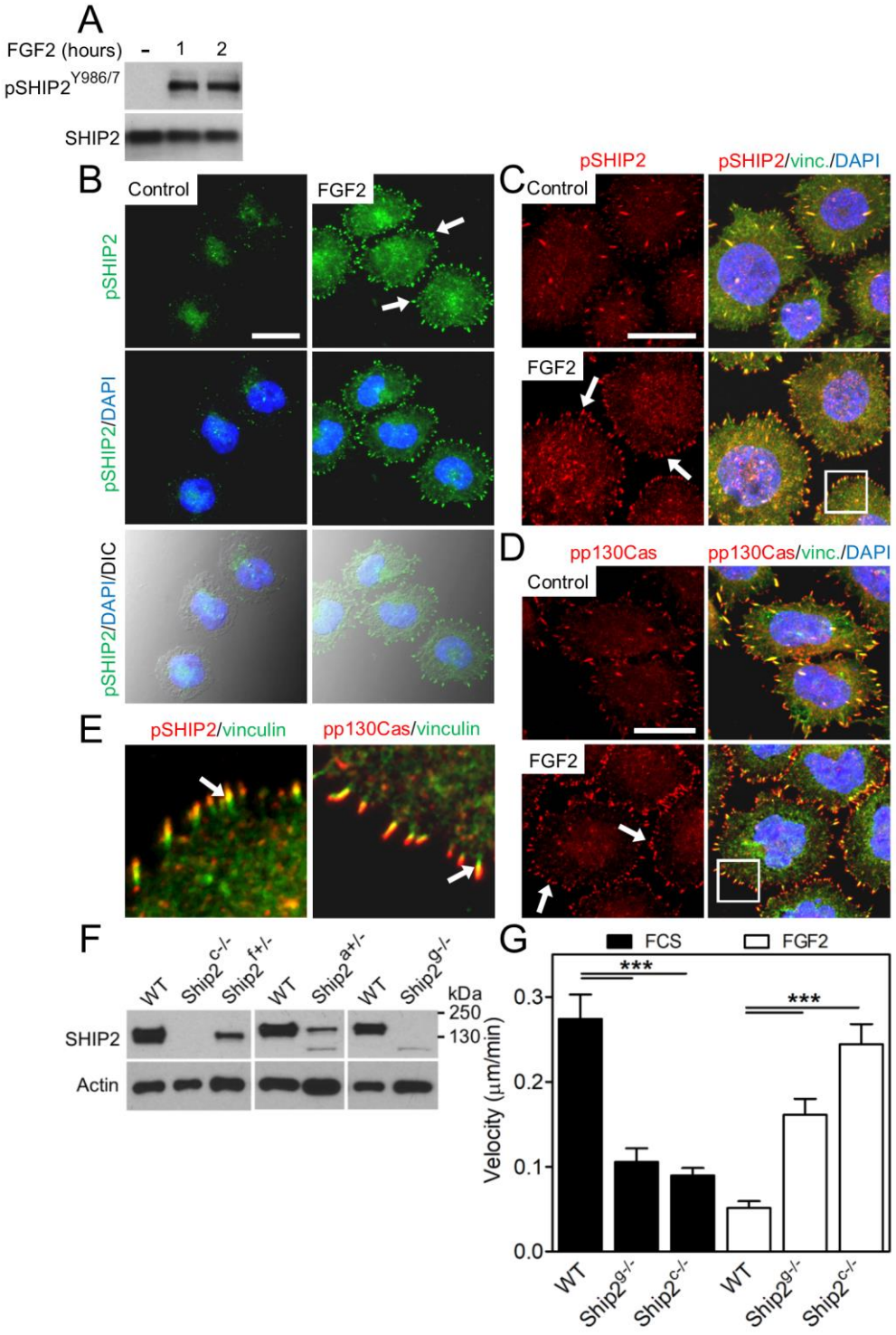
A
FGF2 (hours) - 1 2
pSHIP2Y986/7
SHIP2
B
Control
FGF2
pSHIP2
pSHIP2/DAPI
pSHIP2/DAPI/DIC
C
pSHIP2
pSHIP2/vinc./DAPI
Control
FGF2
D
pp130Cas
pp130Cas/vinc./DAPI
Control
FGF2
E
pSHIP2/vinculin
pp130Cas/vinculin
F
WT
Ship2c-/-
Ship2f+/-
Ship2a+/-
Ship2g-/-
kDa
250
130
SHIP2
Actin
G
FCS
FGF2
***
***
Velocity (μm/min)
0.0
0.1
0.2
0.3
WT
Ship2g-/-
Ship2c-/-
WT
Ship2g-/-
Ship2c-/-

Figure 5

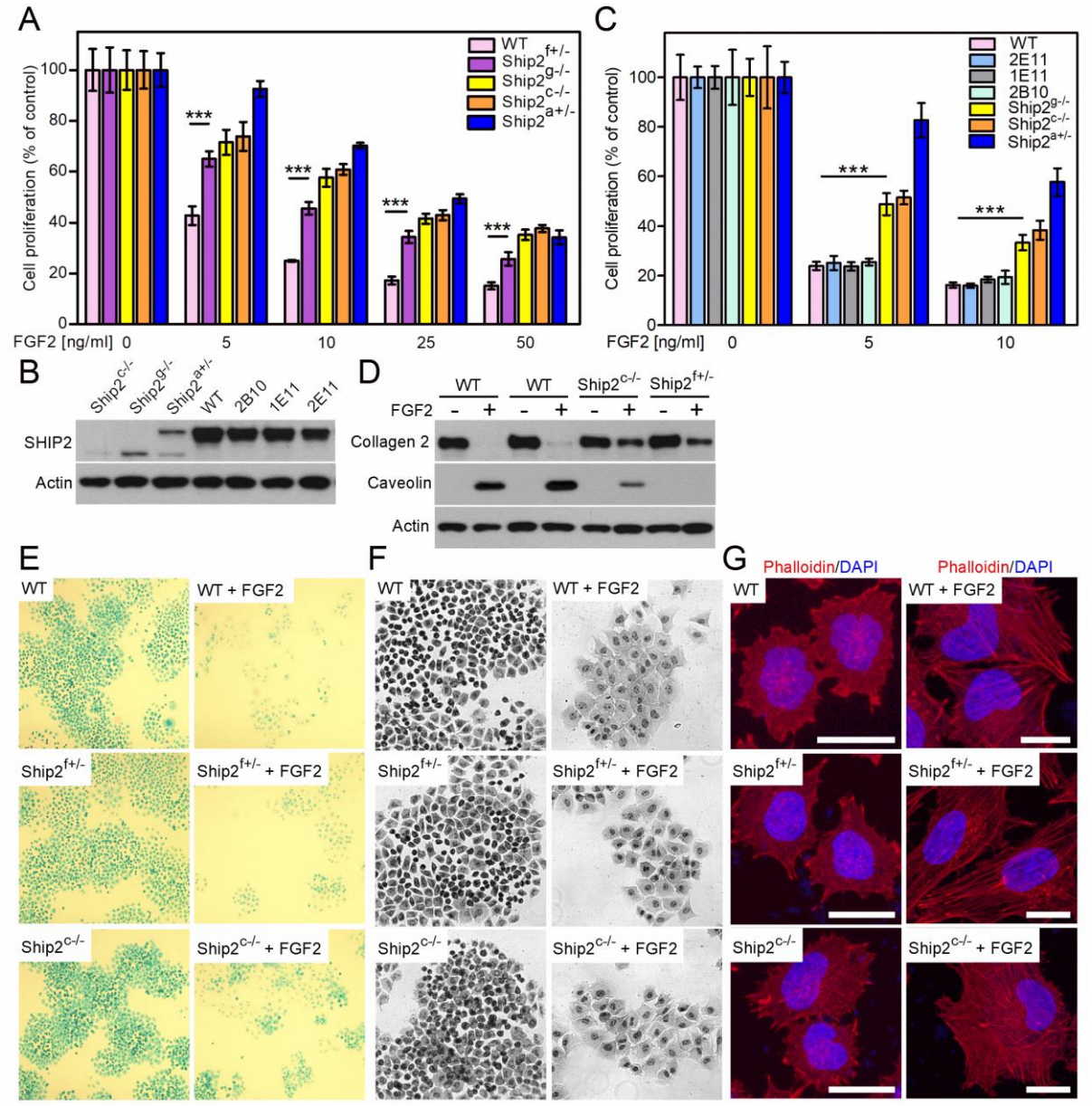
A
Cell proliferation (% of control)
FGF2 [ng/ml] 0 5 10 25 50
WT
Ship2f+/-
Ship2g-/-
Ship2c-/-
Ship2a+/-
***
C
Cell proliferation (% of control)
FGF2 [ng/ml] 0 5 10
WT
2E11
1E11
2B10
Ship2g-/-
Ship2c-/-
Ship2a+/-
***
B
Ship2c-/-
Ship2g-/-
Ship2a+/-
WT
2B10
1E11
2E11
SHIP2
Actin
D
WT
WT
Ship2c-/-
Ship2f+/-
FGF2 - + - + - + - +
Collagen 2
Caveolin
Actin
E
WT
WT + FGF2
Ship2f+/-
Ship2f+/- + FGF2
Ship2c-/-
Ship2c-/- + FGF2
F
WT
WT + FGF2
Ship2f+/-
Ship2f+/- + FGF2
Ship2c-/-
Ship2c-/- + FGF2
G
Phalloidin/DAPI
Phalloidin/DAPI
WT
WT + FGF2
Ship2f+/-
Ship2f+/- + FGF2
Ship2c-/-
Ship2c-/- + FGF2

Figure 6

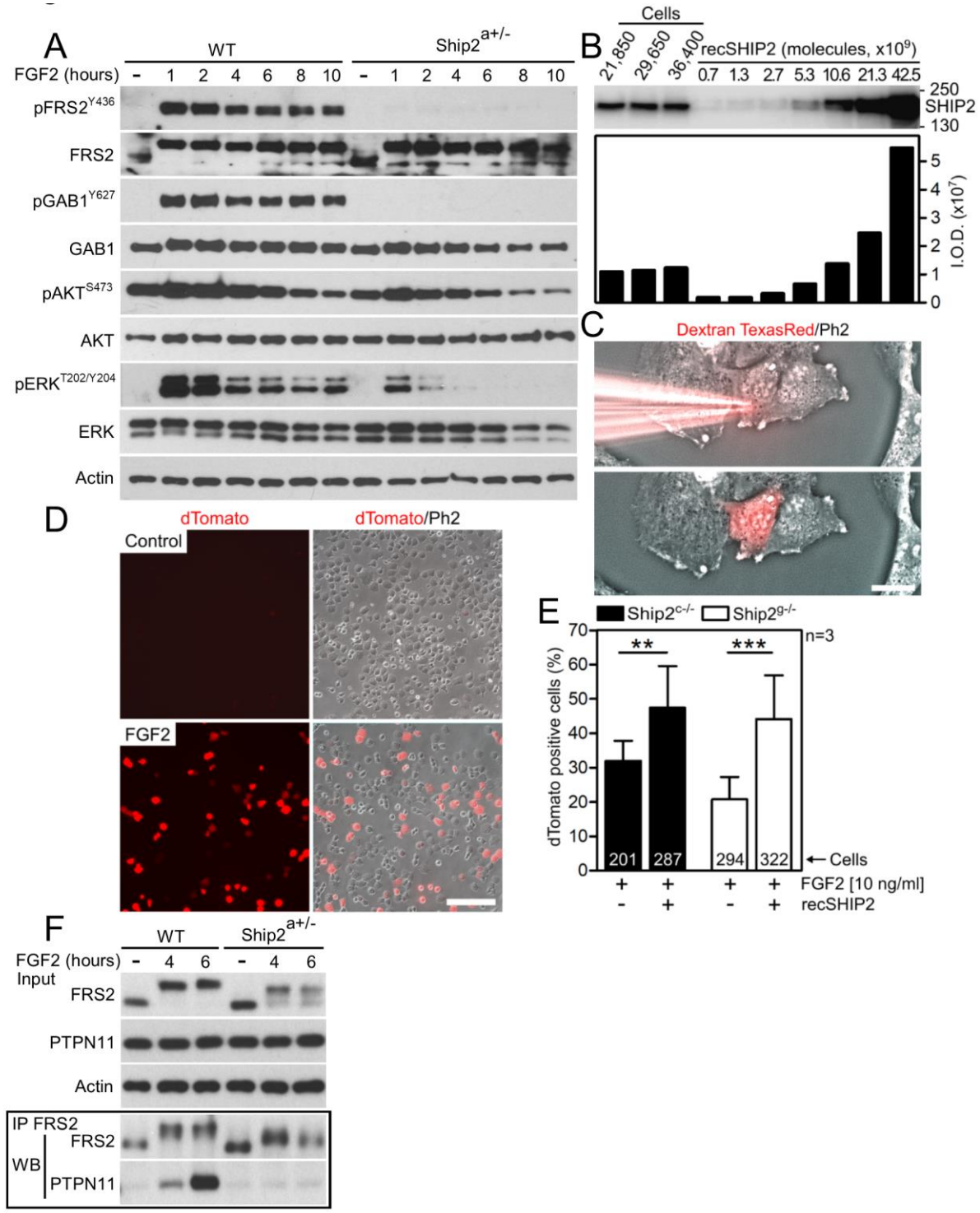
A
WT
Ship2a+/-
FGF2 (hours) - 1 2 4 6 8 10 - 1 2 4 6 8 10
pFRS2Y436
FRS2
pGAB1Y627
GAB1
pAKTS473
AKT
pERKT202/Y204
ERK
Actin
B
Cells
21,850 29,650 36,400
recSHIP2 (molecules, x10^9)
0.7 1.3 2.7 5.3 10.6 21.3 42.5
250
SHIP2
130
I.O.D. (x10^7)
C
Dextran TexasRed/Ph2
D
dTomato
dTomato/Ph2
Control
FGF2
E
Ship2c-/-
Ship2g-/-
n=3
**
***
dTomato positive cells (%)
201 287 294 322
Cells
FGF2 [10 ng/ml]
recSHIP2
F
WT
Ship2a+/-
FGF2 (hours) - 4 6 - 4 6
Input
FRS2
PTPN11
Actin
IP FRS2
WB
FRS2
PTPN11

Figure 7

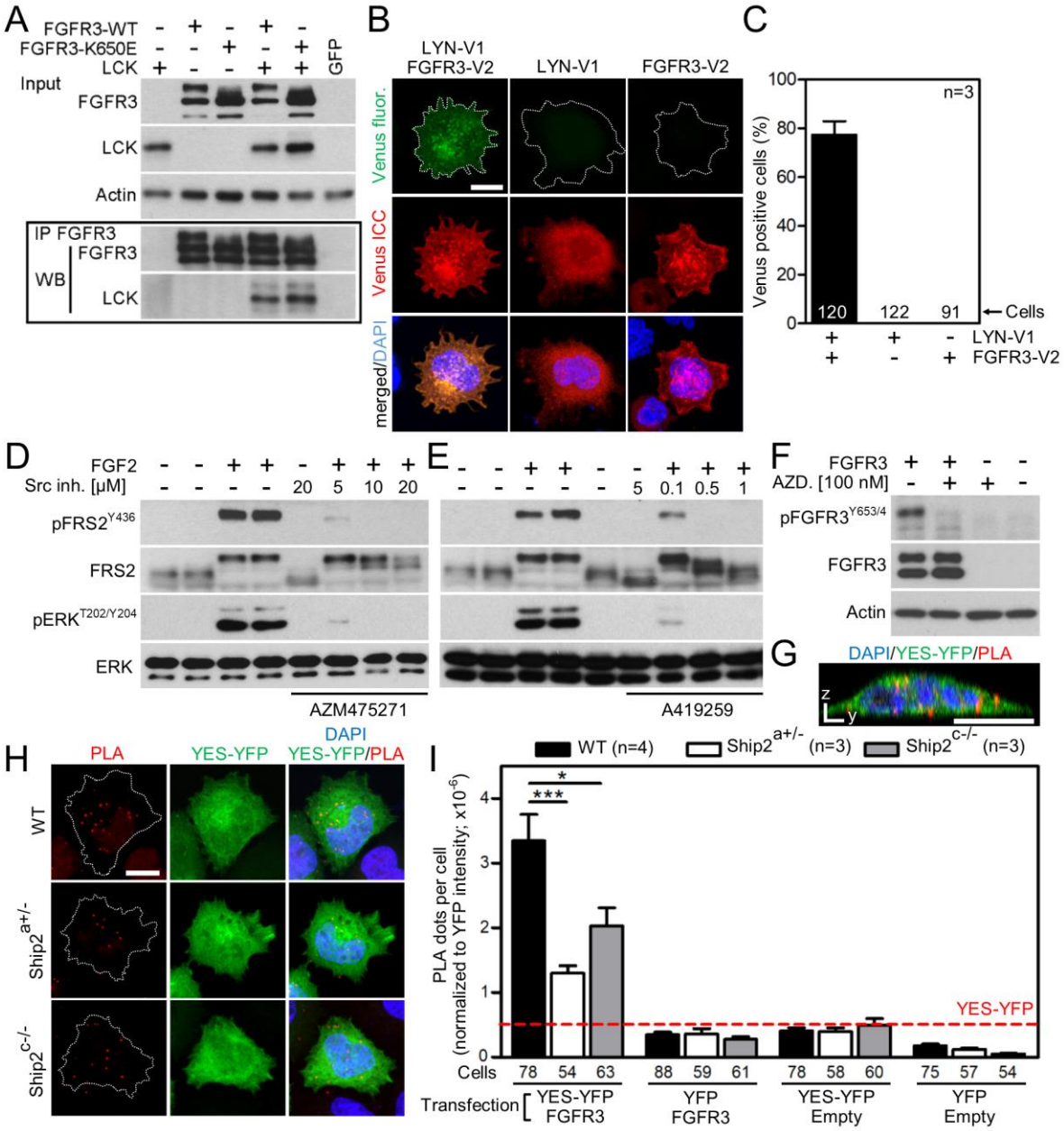
A
FGFR3-WT
FGFR3-K650E
LCK
GFP
Input
FGFR3
LCK
Actin
IP FGFR3
WB
FGFR3
LCK
B
LYN-V1 FGFR3-V2
LYN-V1
FGFR3-V2
Venus fluor.
Venus ICC
merged/DAPI
C
n=3
Venus positive cells (%)
120
122
91
Cells
LYN-V1
FGFR3-V2
D
FGF2
Src inh. [μM]
pFRS2Y436
FRS2
pERKT202/Y204
ERK
AZM475271
E
A419259
F
FGFR3
AZD. [100 nM]
pFGFR3Y653/4
FGFR3
Actin
G
DAPI/YES-YFP/PLA
H
PLA
YES-YFP
DAPI
YES-YFP/PLA
WT
Ship2a+/-
Ship2c-/-
I
WT (n=4)
Ship2a+/- (n=3)
Ship2c-/- (n=3)
PLA dots per cell (normalized to YFP intensity; x10-6)
YES-YFP
Cells
78 54 63
88 59 61
78 58 60
75 57 54
Transfection
YES-YFP FGFR3
YFP FGFR3
YES-YFP Empty
YFP Empty

Figure 8

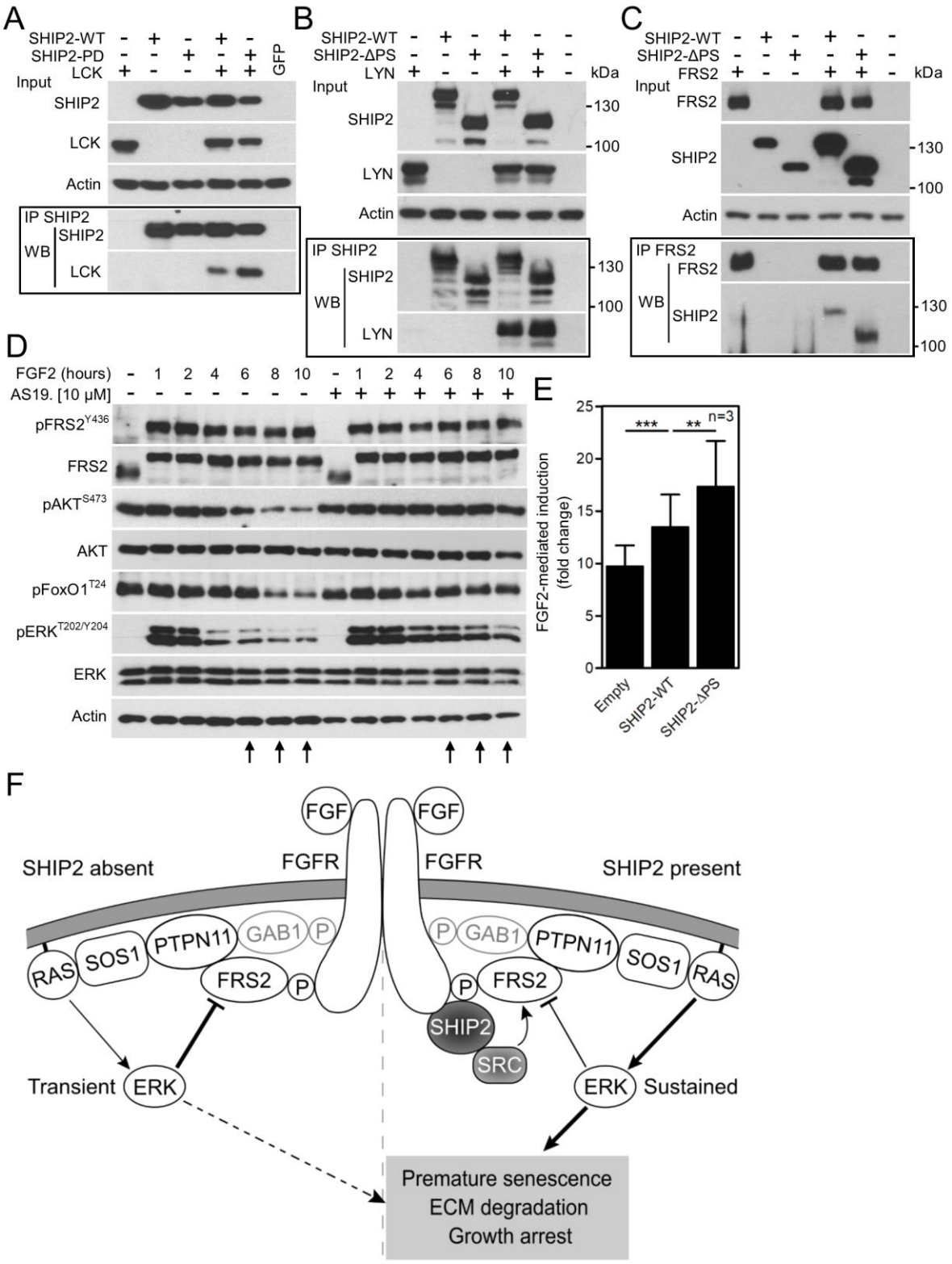
A
SHIP2-WT
SHIP2-PD
LCK
GFP
Input
SHIP2
LCK
Actin
IP SHIP2
WB
SHIP2
LCK
B
SHIP2-WT
SHIP2-ΔPS
LYN
kDa
Input
SHIP2
LYN
Actin
130
100
IP SHIP2
WB
SHIP2
LYN
C
SHIP2-WT
SHIP2-ΔPS
FRS2
kDa
Input
FRS2
SHIP2
Actin
IP FRS2
WB
FRS2
SHIP2
D
FGF2 (hours)
AS19. [10 μM]
pFRS2Y436
FRS2
pAKTS473
AKT
pFoxO1T24
pERKT202/Y204
ERK
Actin
E
FGF2-mediated induction (fold change)
n=3
***
**
Empty
SHIP2-WT
SHIP2-ΔPS
F
SHIP2 absent
SHIP2 present
FGF
FGFR
RAS
SOS1
PTPN11
GAB1
FRS2
P
SHIP2
SRC
Transient
ERK
Sustained
Premature senescence
ECM degradation
Growth arrest

Supplementary figure S1

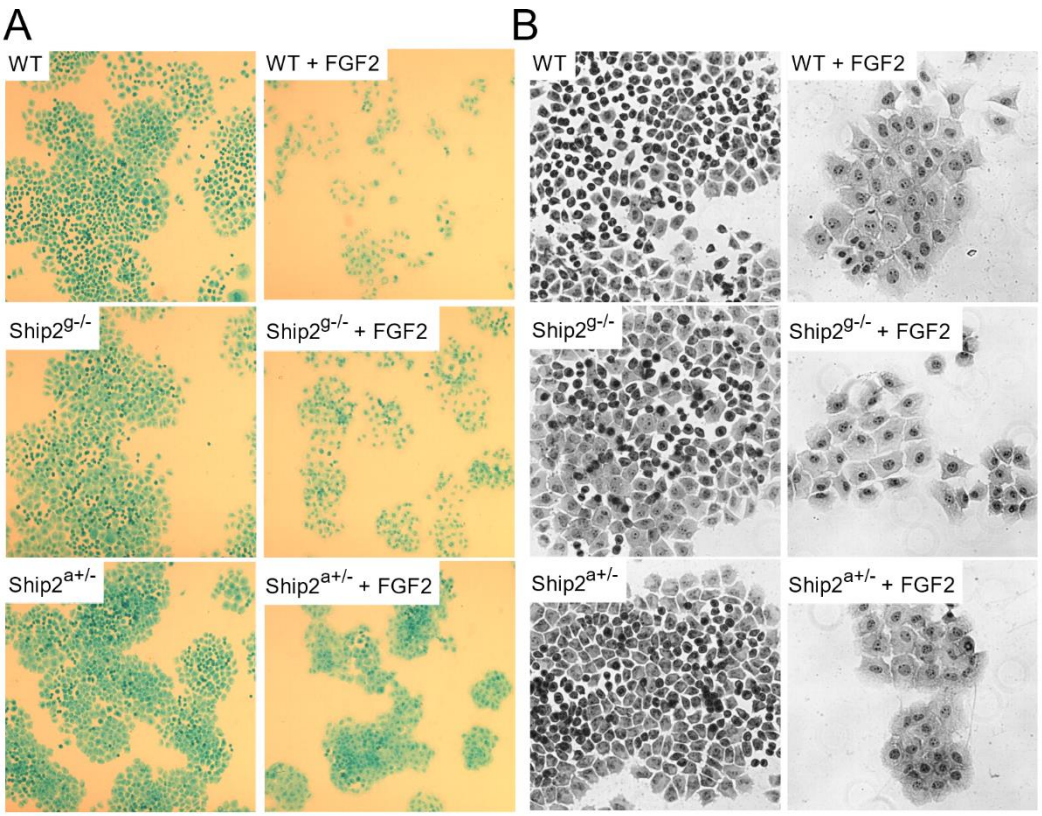

(A) The rescue of FGF2-mediated loss of RCS cartilaginous ECM in two SHIP2^{Crispr} cell lines (Ship2$^{a+/-}$, Ship2$^{g-/-}$), compared to wild-type (WT) RCS cells, visualized by alcian blue staining for sulfated proteoglycans (brightfield, 10x objective). (B) Evidence for spreading in cells treated with FGF2 for 72 hours. This phenotype is not rescued by SHIP2 removal (phase contrast, 20x objective).

Supplementary figure S2

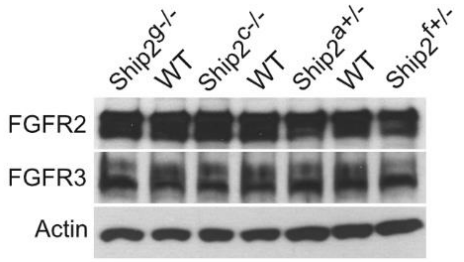

Western blot analysis of endogenous FGFR2 and FGFR3 amount in wildtype RCS cells, and four SHIP2^{Crispr} cell lines.

Supplementary figure S3

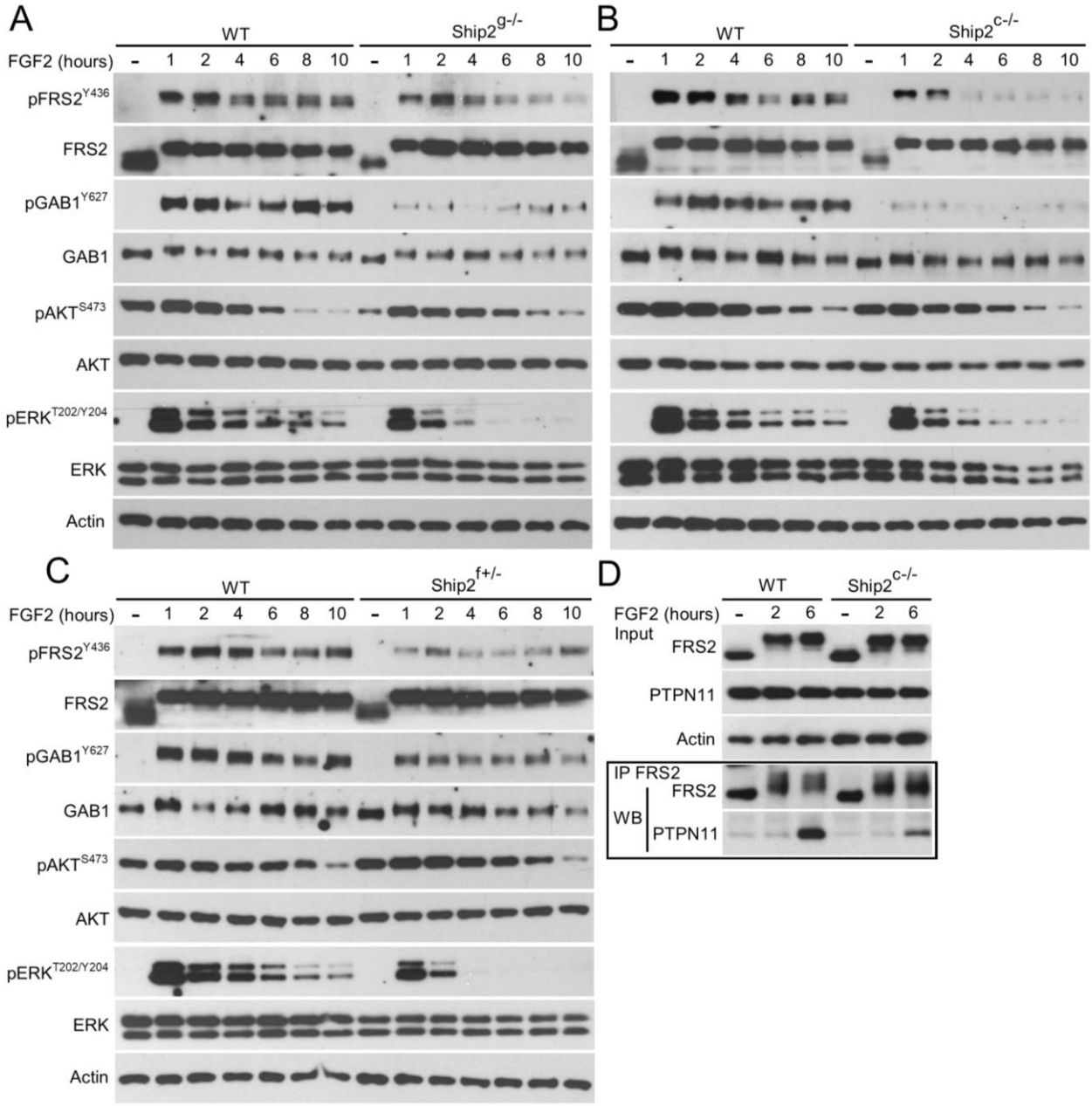

(A-C) Wildtype (WT) and three SHIP2^{Crispr} RCS cell lines (Ship2$^{g-/-}$, Ship2$^{c-/-}$, Ship2$^{f+/-}$) were treated with FGF2 for indicated times and analyzed for phosphorylated (p) forms of FRS2, B1 AKT and ERK by WB. Note the lack of FGF2-mediated FRS2 and GAB1 adapter phosphorylation with corresponding under-phosphorylation of ERK. Actin and total level of given protein serve as loading controls. (D) WT and Ship2$^{c-/-}$ cells were treated with FGF2, FRS2 was immunoprecipitated (IP) and its immunocomplexes analyzed for SHP2 presence by WB. Note the impaired FRS2-SHP2 association in Ship2$^{c-/-}$ cells. Actin serves as quantity control for IP input.

Supplementary figure S4

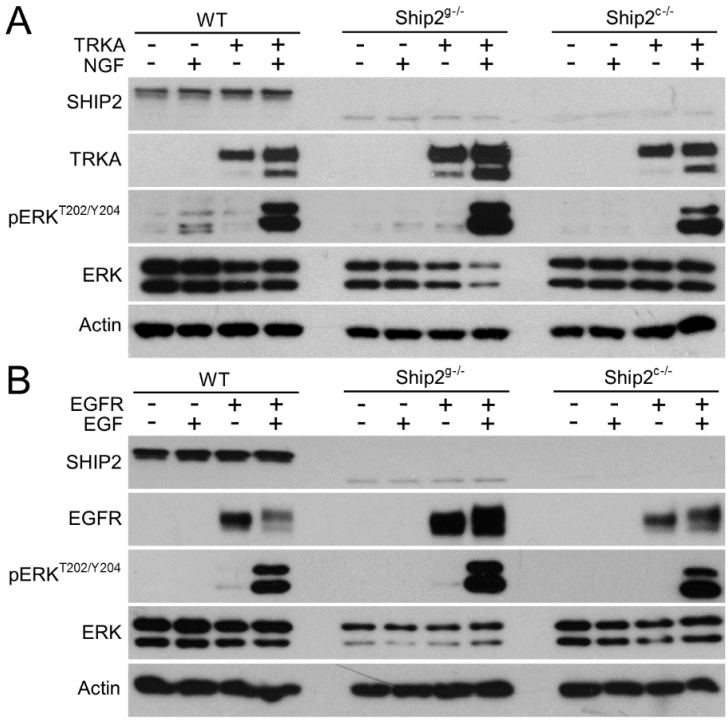

(A, B) Wildtype (WT) RCS cells and two SHIP2^{Crispr} cell lines (Ship2$^{g-/-}$, Ship2$^{c/-}$) were transfected with TRKA or EGFR for 24 hours, treated with NGF (50 ng/ml; 2 hours) or EGF (50 ng/ml; 30 minutes), and analyzed for ERK phosphorylation by western blot. Actin serves as loading control. No substantial impairment of NGF- or EGF-mediated in ERK activity was found in SHIP2^{Crispr} cells.

Supplementary figure S5

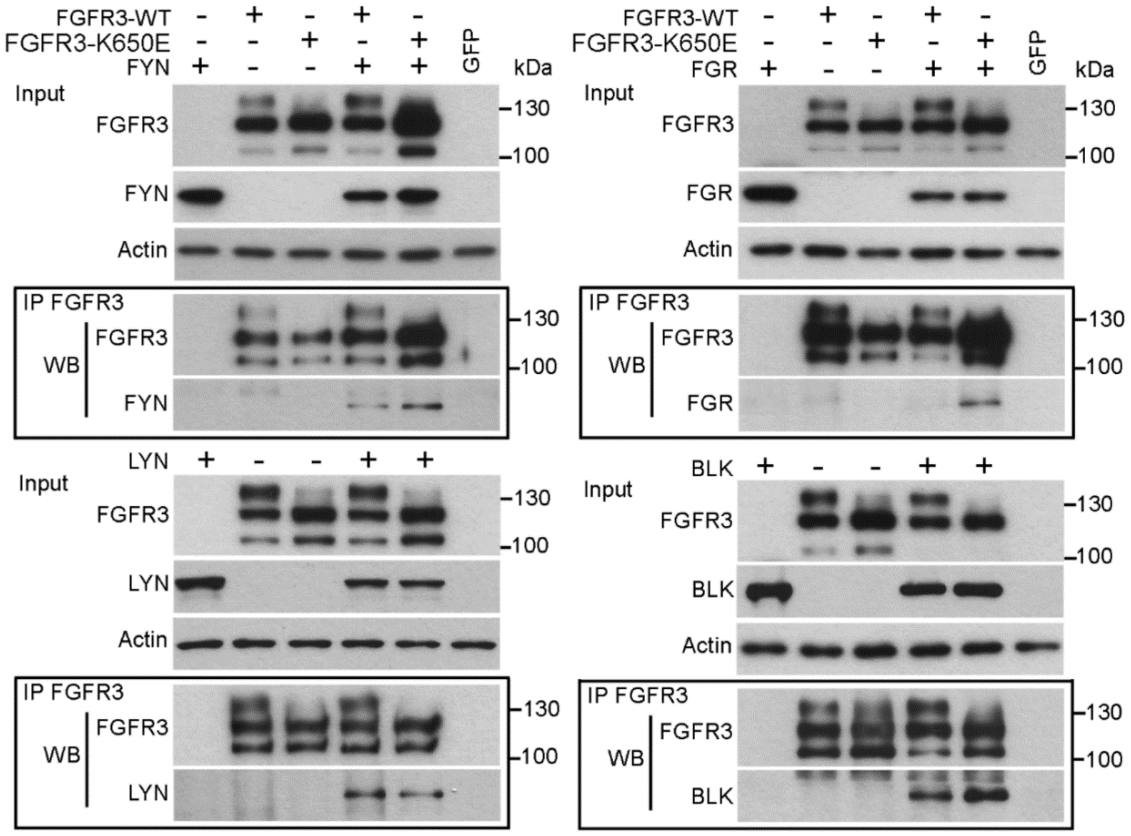

293T cells were transfected with FLAG-tagged wildtype (WT) FGFR3 or K650E FGFR3 together with YFP-tagged FYN, FGR and BLK or HIS-tagged LYN. FGFR3 was immunoprecipitated (IP) 24 hours later and its immunocomplexes were analyzed for FGFR3 and the given SRC kinase by WB. Cells transfected with GFP-expressing vector serve as a control for IP. Actin serves as a loading control for IP input.

Supplementary figure S6

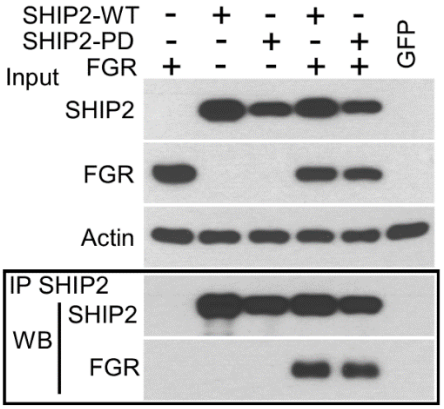

293T cells were transfected with FLAG-tagged SHIP2 and YFP-tagged FGR, SHIP2 was IP-ed 24 hours later and its immunocomplexes analyzed for FGR presence by WB. Note the FGR association with both wild-type (WT) and catalytically-inactive (PD) SHIP2. Cells transfected with GFP plasmid serve as transfection control.

Supplementary table S1: Antibodies used in the study

Antibody *Phosphorylated motif*	*Catalog #*	*Manufacturer*
Actin	3700	Cell Signaling
AKT	9272	Cell Signaling
pAKT^{S473}	4060	Cell Signaling
BLK	3262	Cell Signaling
Caveolin 1	3238	Cell Signaling
Collagen 2	CL50241AP	Cedarlane
ERK	9102	Cell Signaling
pERK$^{T202/Y204}$	4376	Cell Signaling
FLAG	F1804	Sigma-Aldrich
pFGFR$^{Y653/Y654}$	3476	Cell Signaling
FGFR2	sc-122	Santa Cruz Biotechnology
FGFR3	sc-123, sc-13121	Santa Cruz Biotechnology
FGR	2755	Cell Signaling
pFoxO1^{T24}/pFoxO3a^{T72}	9464	Cell Signaling
FRS2	sc-8318	Santa Cruz Biotechnology
pFRS2^{Y436}	3861	Cell Signaling
FYN	4023	Cell Signaling
GAB1	3232	Cell Signaling
pGAB1^{Y627}	3231	Cell Signaling
GFP	sc-53882	Santa Cruz Biotechnology
LCK	2752	Cell Signaling
LYN	2732	Cell Signaling
p130CAS	610271	BD Biosciences
pp130CAS^{Y410}	4011	Cell Signaling
SHIP2	ab166916	Abcam
pSHIP2^{Y497}	NBP2-24461	RnD Systems
pSHIP2$^{Y986/Y987}$	2008	Cell Signaling
pSHIP2^{Y1135}	5445	Cell Signaling
PTPN11	610621	BD Biosciences
V5	R960-25	Invitrogen
Vinculin-FITC	F7053	Sigma-Aldrich
pY (4G10)	05-321	Millipore

Supplementary table S2: Expression vectors used in the study

To all – please check this carefully

Vector	*Insert*	*Backbone*	*Source/Reference*
Lyn D	Lyn (Δ67-218aa)	pDEST26	Origene
Lyn DD	Lyn (Δ127-218aa)	pDEST26	Origene
P37L	Venus V1 with Linker	pDEST-ORF-V1	Addgene
P38L	Venus V2 with Linker	pDEST-ORF-V2	Addgene
Lyn-V1	Lyn-Venus 1	P37L	Addgene, customized
FGFR3-V2	FGFR3-Venus 2	P38L	Addgene, customized
SHIP2-WT	SHIP2-V5	pCMV6-Entry-Myc-DDK	Origene
SHIP2-ΔPS	SHIP2(Δ419-739aa)-V5	pCMV6-Entry-Myc-DDK	Origene
SHIP2-ΔPR1	SHIP2(Δ123-410aa)-V5	pCMV6-Entry-Myc-DDK	Origene
SHIP2-N1	SHIP2(Δ419-1258aa)-V5	pCMV6-Entry-Myc-DDK	Origene
SHIP2-N2	SHIP2(Δ1-122, 419-1258aa)-V5	pCMV6-Entry-Myc-DDK	Origene
SHIP2-C1	SHIP2-V5 (Δ1-739aa)	pCMV6-Entry-Myc-DDK	Origene
SHIP2-C2	SHIP2-V5 (Δ1-739, 1190-1258aa)	pCMV6-Entry-Myc-DDK	Origene
SHIP2-PD	SHIP2-V5 (P686A, D690A, R691A)	pCMV6-Entry-Myc-DDK	Origene
SHIP2-WT	SHIP2	pCR3.1-FLAG	Invitrogen
TRKA	TRKA-V5	pDEST26-His6	Gudernova et al., 2017 all eLIFE
EGFR	EGFR-V5	pDEST26-His6	Gudernova et al., 2017
FGFR3	FGFR3-V5	pcDNA3.1/V5-His	Gudernova et al., 2017
FGFR3-K650M	FGFR3-K650M-V5	pcDNA3.1/V5-His	Gudernova et al., 2017
FGFR3-K650E	FGFR3-K650E-FLAG	pRK7	Krejci et al., 2007, JBC
FGFR3-K508M	FGFR3-508M-FLAG	pRK7	Krejci et al., 2007, JBC
YES-YFP	YES-YFP	pdEYFP-Clamp-YFP	ImaGenes
LCK	LCK	pDEST26-His6	ImaGenes
LYN	LYN	pDEST26-His6	ImaGenes
FYN-YFP	FYN-YFP	pdEYFP-Clamp-YFP	ImaGenes
FGR-YFP	FGR-YFP	pdEYFP-Clamp-YFP	ImaGenes
BLK-YFP	BLK-YFP	pdEYFP-Clamp-YFP	ImaGenes
FRS2	FRS2-FLAG	….	Origene
EYFP			Clontech